

FC
689

Reprinted from Transactions of the SPWLA Seventeenth Annual Logging Symposium
June 9-12, 1976, Denver, Colorado.

THEORY AND APPLICATIONS OF THE BOREHOLE AUDIO TRACER SURVEY

E. L. Britt

GO International, Inc.
Ft. Worth, Texas

UNIVERSITY OF UTAH
RESEARCH INSTITUTE
EARTH SCIENCE LAB.

ABSTRACT

The Borehole Audio Tracer Survey (BATS or sound survey) is a new surveying device which can be used to locate and quantify fluid flow outside of casing. Additionally the sound* logger can be utilized as a flowmeter (without moving parts) to measure fluid flowing past the tool.

Part I illustrates use of the BATS log to locate and evaluate the quantity of fluid flow outside of casing. It is demonstrated that an index of flow magnitude can be determined and, as a result, a monetary value can be placed on this lost production.

Part II demonstrates the use of the BATS log to determine the relative flow rate of individual perforations in limited entry completion, where mass flow rate through the perforation is sufficient to produce turbulent flow. An additional technique for evaluating perforated zones (e.g. 4 per ft., etc.) is also shown.

Part III demonstrates use of the BATS device as a downhole flowmeter having no moving parts. It is shown that the BATS device, unlike mechanical flowmeters, can, under favorable circumstances, identify the type of fluid flowing (e.g. liquid, liquid-gas, or foam) as well as the flow rate.

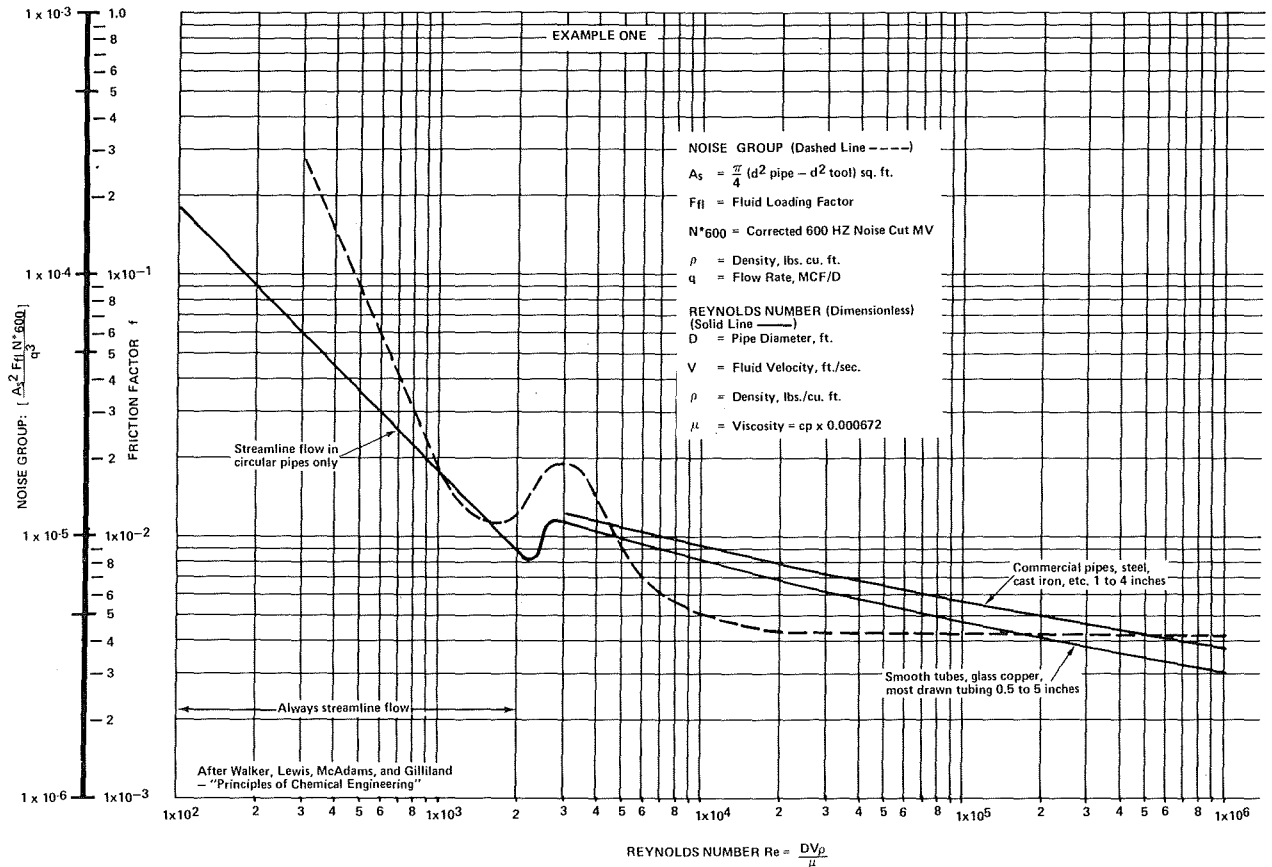
INTRODUCTION

Since the Borehole Audio Tracer Survey is a new log to most interpreters, a description of the equipment, logging technique, and a brief theoretical explanation will be given. Additionally, two required corrections to observed log values will be explained.

Equipment - The downhole tool is 1 11/16" in diameter and 48" long with a 15,000 psi and 350°F temperature rating. It can be run in conjunction with a temperature device to provide sequential surveys on a single trip in the hole. A very useful combination is the temperature and sound logger both recorded under shut-in and flowing conditions.

The downhole tool is simply a very sensitive microphone with a downhole amplifier. The transducer is designed to respond to sound which originates in any direction around the well and therefore has no directional properties. The tool is run without centralizers since the proper tool response depends strongly

*In this paper the generic term sound device will be used in place of BATS Log or logger.



dealing with flow in an annulus whereas circular pipes present a clear unrestricted diameter for full development of laminar flow.

For a complete theoretical explanation of how sound frequencies can be used to determine flow, the reader is referred to the following paper: "The Structure and Interpretation of Noise From Flow Behind Cemented Casing" by R. M. McKinley, F. M. Bower, and R. C. Rumble. SPE #3999 J.P.T.

Additionally, all of the correlations used in this paper were developed by Dr. R. M. McKinley and his release for publication is hereby gratefully acknowledged.

CORRECTIONS TO LOG RECORDED VALUES

Two corrections must be made to all log values before entering the various Noise Level or Noise Group vs. Flow Rate Charts. They are:

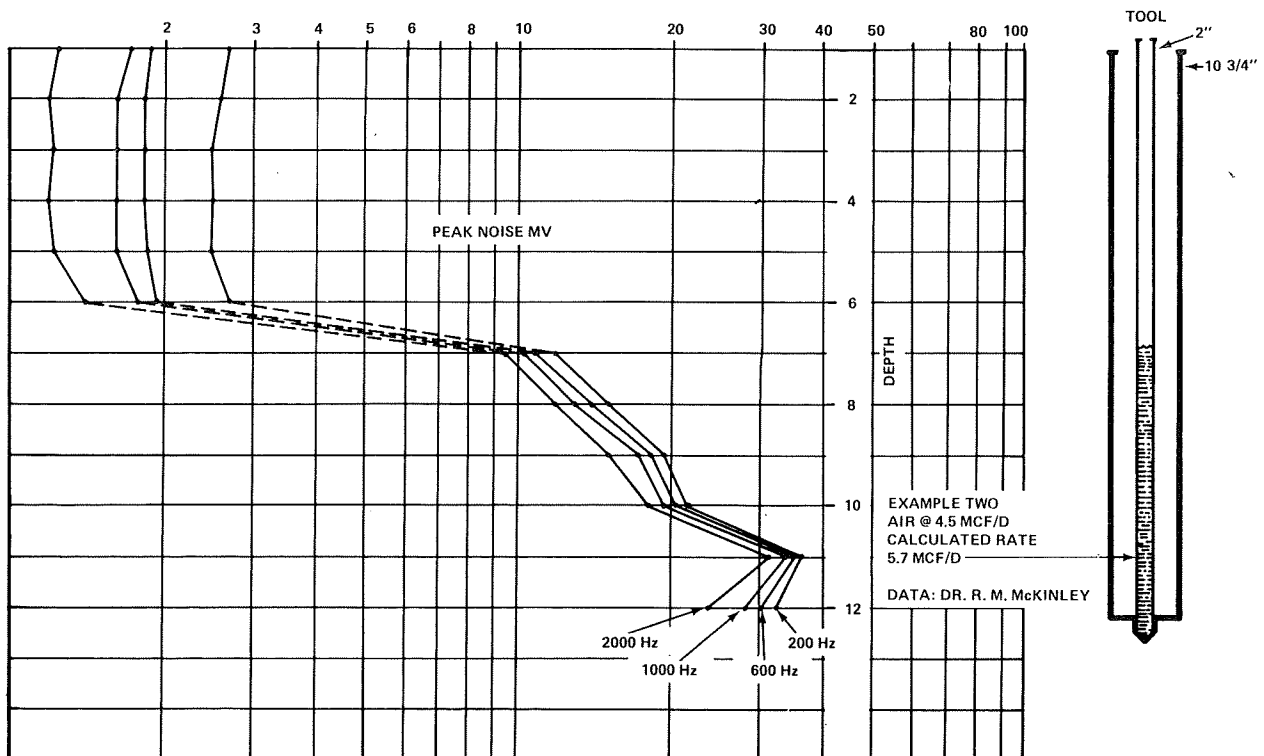
- A. Cable Corrections: All noise log signals are subject to attenuation between the downhole tool and the surface. Figures 1 and 2 provide the amount of correction which must be applied to each frequency for the type and cable lengths, used to record the survey. For cable diameters 5/16" and greater use the corrections from Figure 1. For cable diameters 7/32" and less use the corrections from Figure 2. Please note that the corrections can be quite large, especially considering the higher frequencies

when recorded on long, small diameter cable.

B. Geometry Corrections: The Flow Rate Estimation Charts (Figures 3 and 4)* are for a specific type of wellbore geometry. First, the tool must be in liquid for the proper crystal loading. Second, the leak must be located behind the pipe in which the tool is located; that is, the sonde is shielded from the noise source by one pipe string. For this situation, the geometric factor is unity. This base case is referred to as a "tubingless completion" on Figures 1 and 2, since this is the most typical type completion in which only one pipe string will be between the sonde and the leak.

The factors (F_g) listed depend strongly upon the actual degree of metal to metal coupling between the sonde and tubing or casing wall; consequently, they should be regarded as approximate values only.

In a later section F_g (or its equivalent F_{f1}) will be derived in a different manner for the case where fluid flowing in contact with the sound tool is solely responsible for the noise recorded.



*All correlations of measured signal vs. flow rate, F_g , etc., in this paper are valid only for GO International equipment.

LABORATORY EXPERIMENTS

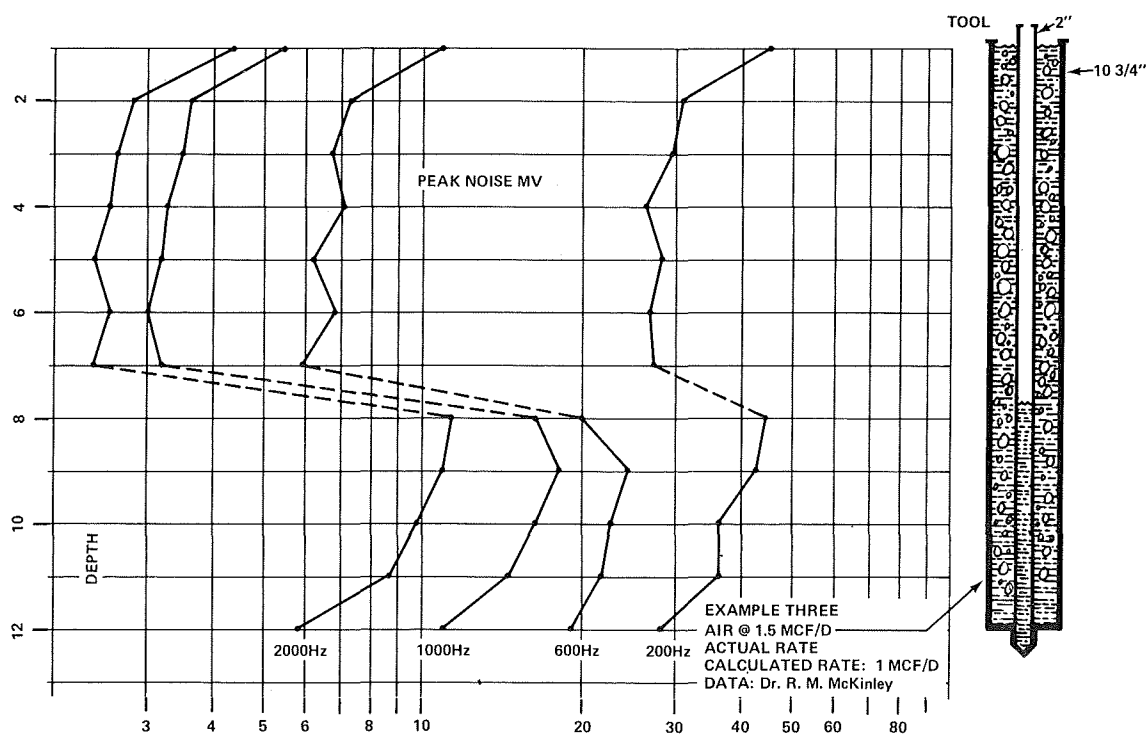
Two of the many laboratory experiments conducted in this research project will be described. These experiments will aid in understanding some of the characteristics of field logs and demonstrate how the empirical relationship of sound vs. flow was developed.

EXAMPLE 2

Example 2 shows the sound spectrum and amplitude recorded when the fluid flowing is single phase and gas. The mechanical diagram on the right indicates that the annulus is filled with gas (actually air, at or near atmospheric pressure) and the tubing string is filled with liquid to a depth of seven feet. Air at 100 psi is throttling into the annulus at a depth of eleven feet.

Note that all of the frequency cuts are reading essentially the same value at eleven feet. This response is quite typical of single phase gas flow and indicates that most of the noise energy occurs in the higher frequency bands (e.g. 1000Hz and 2000Hz). From eleven feet to seven feet the noise levels decline in value rather slowly. When the noise tool leaves the liquid filled section of the tubing, a sharp decrease in signal amplitude is recorded; this is a consequence of the change in crystal loading which affects sound coupling to the tool. This liquid level response is routinely observed on field logs.

Above the liquid level all frequency cuts are quite low in magnitude as a consequence of gas being the sound coupling fluid in both tubing and annulus.



EXAMPLE 3

Example 3 shows the sound spectrum and amplitude recorded when the fluid flow is two phase, gas flowing through liquid. Again the mechanical diagram on the right indicates the fluid levels, with air at 100 psi throttling into the annulus at a depth of eleven feet.

Note the curve separation between frequency cuts which exists throughout this experiment. This is the typical response of two phase flow (gas flowing through liquid); such flow generates the turning, roiling, shredding, and bubbling with the largest portion of total energy confined to the 200Hz and 600Hz range. Note again the sharp reduction in tool response above seven feet caused by the tool leaving liquid couplings. The 200Hz does not decline in amplitude as sharply as do the other frequency cuts. This phenomenon is caused by the non-typical (of field conditions) nature of the experiment. The tubing is not damped mechanically (e.g. against casing, etc.) as does occur in actual practice; hence the abnormally high 200Hz amplitude above the tubing liquid level.

The results of flow calculations are shown on each example. The point here is to note that flow rates determined from sound logs are accurate only within a factor range of two. This means that the actual flow rate can range between twice and one half the calculated value.

PART I - DETECTION OF FLUID FLOW OUTSIDE OF CASING AND FLOW RATE ESTIMATION

EXAMPLE 4

Example 4 is a sand-shale sequence recording from the Texas Gulf Coast. Zones K-2, K-3 and L-1 have been depleted by previous production. The current production objective is the N-4 zone which is a known gas bearing reservoir. No obvious surface manifestation of downhole problems existed (e.g. pressure on surface casing or annulus, etc.). A problem was suspected since flow rates and pressures were not quite as expected when compared to other wells in the field.

The well was shut-in and a sound log was recorded. Well and logging conditions were as follows:

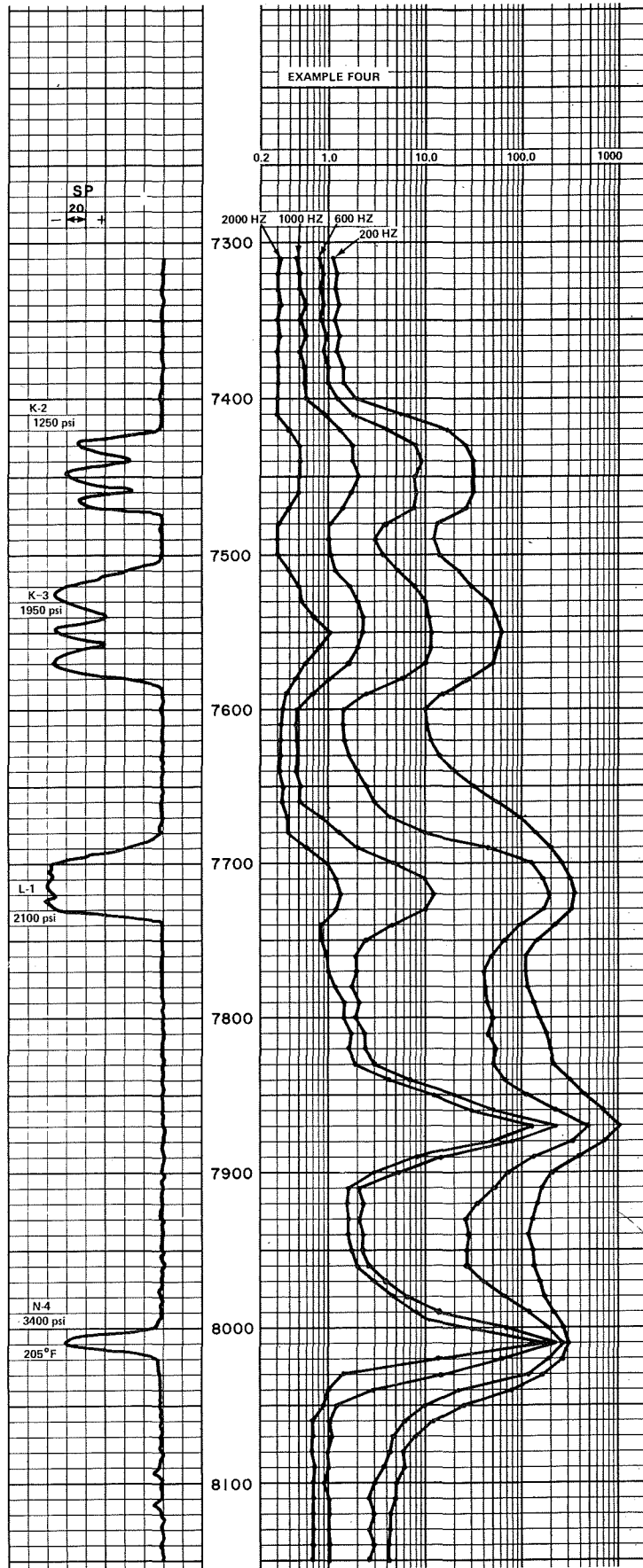
Fluid in annulus; gas in tubing - surface pressure 2900 psi.

Log recorded with 23,500' of 5/16" cable.

Cable factor corrections, from Figure 1:

$$CF_{200Hz} = 1.12; CF_{600Hz} = 1.25; CF_{1000Hz} = 1.45; CF_{2000Hz} = 1.85.$$

The log shows several peaks indicating high sound levels, the highest of which occurs at 7870'. Sound levels above and below the obvious sound peaks are quite low; from this evidence it is reasonably safe to conclude that the well problems were confined to the section shown on the log. The highest sound level at 7870' likely corresponds to a very small restriction in the annular flow path. Thus, the highest sound level does not always correspond to the source or sink for flow.



The source of gas flow in the lower part of the well is the N-4 reservoir at 8008'. Gas is flowing from this reservoir to the depleted reservoir L-1 below 7700'. Flow rate estimation is as follows:

A. Cable Corrections: Log values recorded at the N-4 reservoir are:

$$N_{200} = 300_{MV}, N_{600} = 270_{MV}, N_{1000} = 231_{MV}, \text{ and } N_{2000} = 181_{MV}.$$

Using the cable corrections stated above, corrected values of noise levels (denoted N^*) are:

$$N^*_{200} = (300)(1.12) = 336$$

$$N^*_{600} = (270)(1.25) = 337$$

$$N^*_{1000} = (231)(1.45) = 335$$

$$N^*_{2000} = (181)(1.85) = 335$$

Note that all corrected values are virtually equal; this is the usual indication that the fluid flow is single phase. The fact that N^*_{600} is higher than N^*_{200} is of no significance despite the fact that theoretically it cannot occur. Such differences are caused by the accuracy limitations of commercial electronic equipment and do not invalidate the resultant flow rate calculations.

B. Well Geometry Factor: From the stated well conditions the sound tool is below the packer and the tubing contains gas (no fluid level). Accordingly the well geometrical factor F_g is 2.

C. Flow Rate at 8008': Since the flow is single phase and gas, the N^*_{1000Hz} value is used for flow calculations. N^*_{1000Hz} corrected for cable and F_g is:

$$N^*_{1000Hz} \times F_g = (335)(2) = 670_{MV}.$$

Flow rate cannot be obtained from Figure 4 since the value (670MV) is above the chart range. Flow rate was computed from the formula:

$$q \times \Delta P = 24 (N^*_{1000Hz} - 1.5) \text{ psi MCF/d}$$

$$\therefore q \times \Delta P = (24)(670 - 1.5) \text{ psi MCF/d} = 16.0 \text{ psi MMCF/d.}$$

ΔP is known since the reservoir pressure of both zones is known;

$$\Delta P = (3400 - 2100) \text{ psi} = 1300 \text{ psi}$$

$$\therefore q = \frac{16.0 \text{ psi MMCF/d}}{1300 \text{ psi}} = 12.3 \text{ MCF/d.}$$

This flow rate is at downhole conditions and therefore must be corrected to standard conditions. The reservoir pressure (3400 psi) and temperature (205°F) are known: using the Sp.Gr. = 0.8 correlation of Figure 6 the volume correction factor is 205. Flow rate at standard conditions is:

$$q_{std} = (12.3 \text{ MCF/d})(205) = 2521 \text{ MSCF/d or } 2.5 \text{ MMSCF/d.}$$

The limits of accuracy on this measurement are $\times 2$ and $\div 2$; accordingly the upper and lower limits of the flow rate are:

upper limit: 5 MMSCF/d
lower limit: 1.25 MMSCF/d

Gas from this well is sold for \$1.50/MCF; thus the estimated revenue loss is:

upper limit: \$7500.00/day
lower limit: \$1875.00/day

Such daily dollar loss estimates should prove valuable in the financial justification of workover operations. One of the prime values of the sound logger is the ability to make quantitative estimates of flow and thus to place a dollar value on the lost production.

- D. Flow Rate at 7550': Sound generated at 7550' has all of the typical characteristics of a downhole dump flow. Fluid is moving from the K-3 to the K-2 sand and, since there is a wide difference of magnitude in the frequency cuts, the flow is two phase - gas flowing through water. Flow calculations are as follows:

$$N^*_{200} = (60)(1.12) = 67\text{MV}; N^*_{600} = (12)(1.25) = 15\text{MV}$$

$$\Delta^* = N^*_{200} - N^*_{600} = 52\text{MV}; \Delta^*F_g = (52)(2) = 104\text{MV}$$

$$\text{From Figure 3 } q = \frac{\Delta^*F_g - 6}{9.1} = \frac{104 - 6}{9.1} = 10.77 \text{ MCF/d}$$

From Figure 6, the volume factor is 130 for 200°F, 1950 psi, and Sp.Gr. -0.8. Accordingly, q_{std} is:

$$q_{\text{std}} = (10.77 \text{ MCF/d})(130) = 1400 \text{ MSCF/d or } 1.4 \text{ MMSCF/d}$$

It is not necessary to estimate a pressure drop for two phase flow since the turning, roiling, and shredding of the moving fluid dissipates any pressure differential more or less uniformly throughout the flow path.

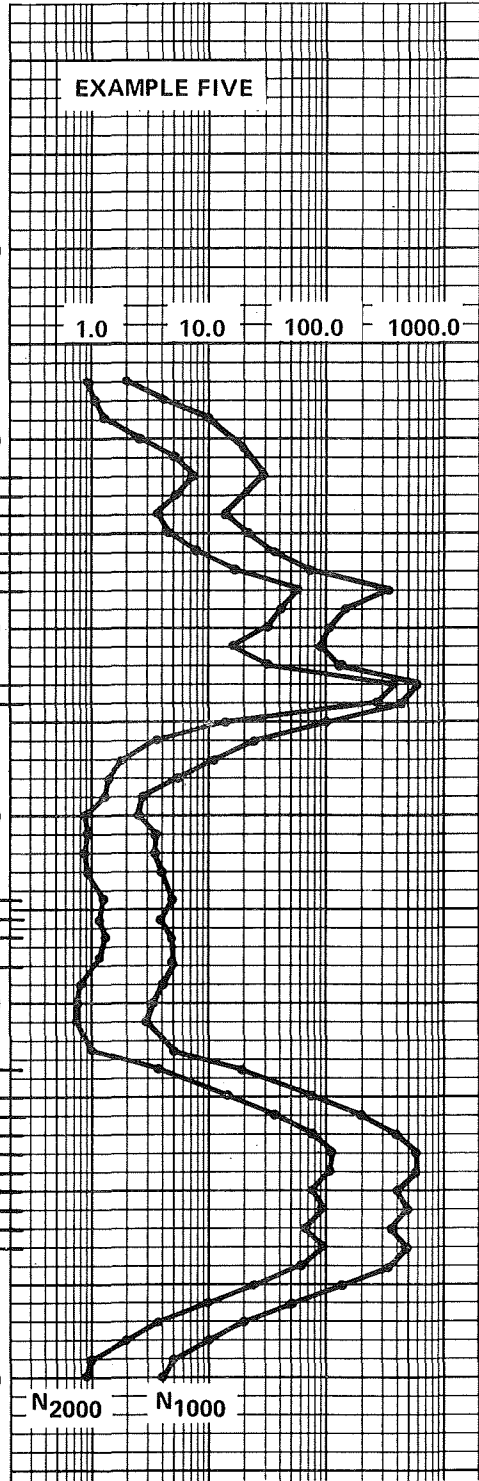
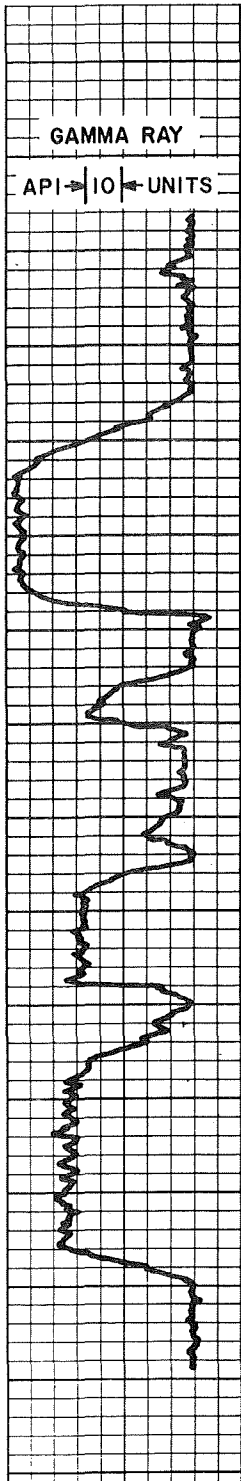
PART II - FLOW RATE EFFICIENCY OF PERFORATIONS

Two interpretation techniques associated with the sound logger can be used to evaluate production efficiency of perforations. These techniques permit allocation of known surface production to individual perforations (limited entry) or perforated zones.

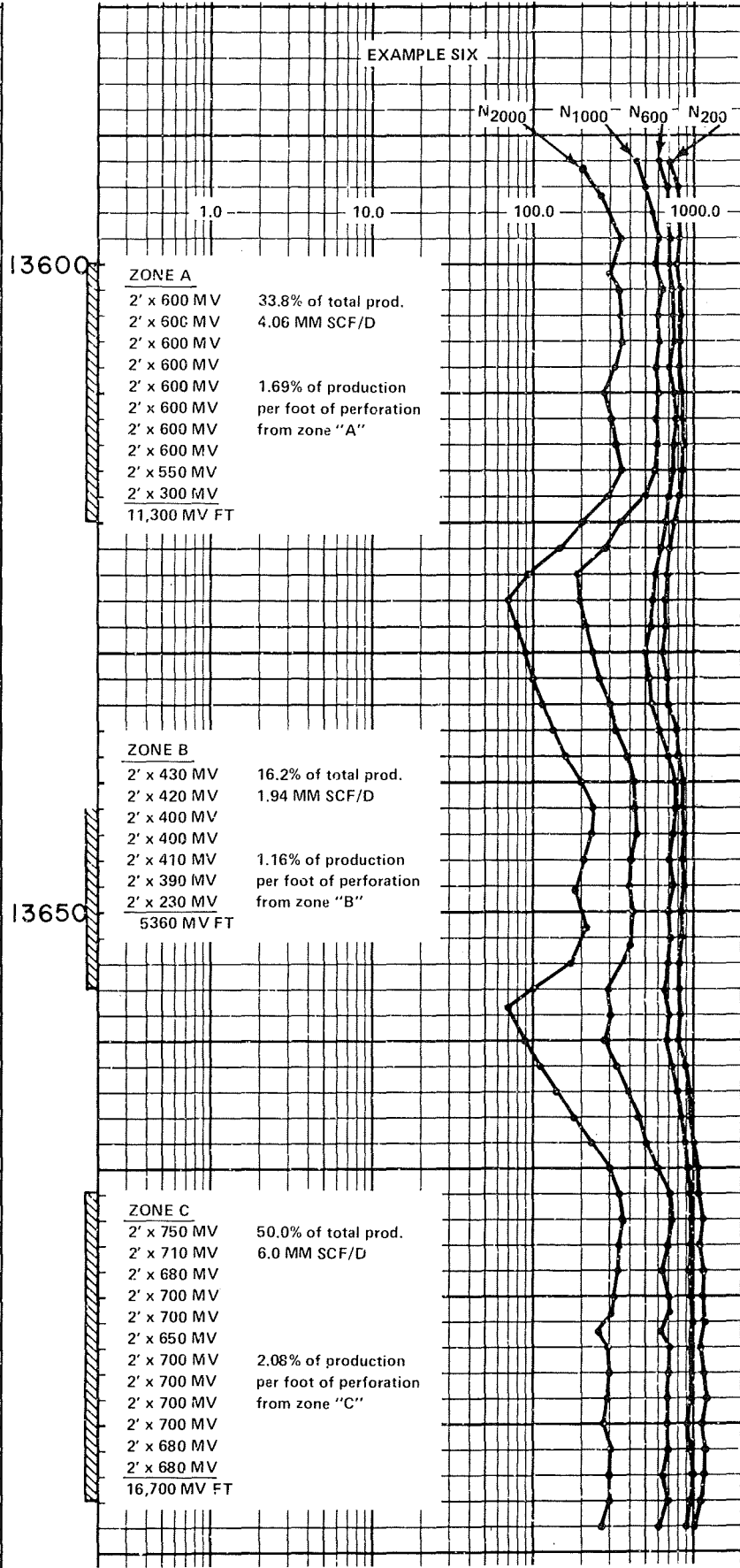
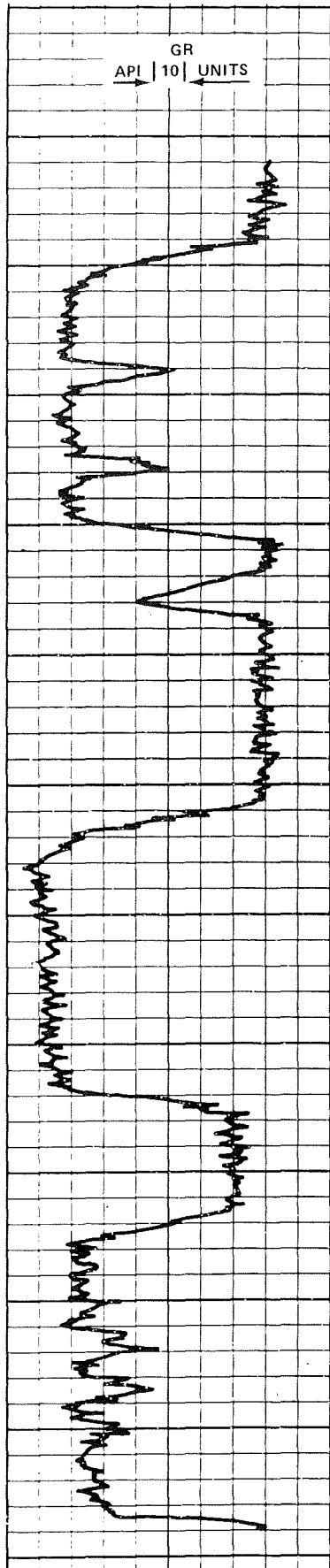
- A. For deep, unplugged perforation, the noise produced by fluid jetting onto the tool from the perforation is related to the production rate, q_p , from the perforation and the perforation diameter D_p by the expression:

$$N_{1000} \approx \frac{q_p^3}{D_p} ; q_p \approx N_{1000}^{1/3}$$

It is therefore only necessary to take the cube root of the N_{1000} Hz noise levels of all perforations to determine relative production. Since the noise values will be used in ratio, it is not necessary to correct for signal losses in the cable. Of course, this analysis also makes the assumption that all perforations have equal diameters, and that the pressure



N1000	$\sqrt[3]{N1000}$	PRODUCTION SHARE
30	3.11	
20	2.71	Zone A
13	2.35	
20	2.71	24.3%
36	3.30	
80	4.31	
330	6.91	
	<u>25.40</u>	
600	8.43	Zone B
430	7.55	5.1%
	<u>15.98*</u>	
	5.33	
*Zone total of 15.98 reduced to 5.33 due to water production.		
5	1.71	Zone C
4	1.59	
5	1.71	
5	1.71	6.4%
	<u>6.72</u>	
20	2.71	Zone D
80	4.31	
200	5.85	
400	7.37	
600	8.43	
600	8.43	
400	7.37	
500	7.94	
330	6.91	
500	7.94	64.2%
	<u>67.26</u>	
TOTAL	104.71	



drop through each perforation is essentially the same. Note also that the logging technique for this type of survey requires that the tool be positioned directly in the center of the flow stream emanating from the perforation.

EXAMPLE 5

This example is a typical well completed in the tight sandstones of New Mexico and Colorado. It was expected to produce about 2 MMSCF/d, actual production was 500 MSCF/d with 200 bbls/d water.

The best producing intervals are obvious by examination of the $N_{1000\text{Hz}}$ signal levels. Zone A appears to be inadequately fractured since it is producing only 25% of the total production. Zone C, like Zone A appears to have missed being fractured.

Note how the $N_{2000\text{Hz}}$ approaches the value of $N_{1000\text{Hz}}$ in Zone B. This is caused by water "bullets" striking the sonde from these perforations. When making an allocation of production from this zone the MV total should be reduced by a factor of three since the $N_{1000\text{Hz}}$ sound level is increased by the water flow. Values of $(N_{1000})^{1/3}$ are tabulated for each zone in this example. This analysis technique is reliable for limited entry perforations and for any zone where the individual perforations can be recognized on the sound log. In such cases the gas expansion is taking place at the perforation. Of course, the flow rate must be high enough to be turbulent through the opening in the casing.

- B. For producing zones which are perforated with two or more shots per foot a different technique must be used. Observation of field logs suggests that fracturing of the cement sheath takes place at the time of perforating; thus gas expansion takes place in the cement sheath instead of the perforations.

The analysis technique uses the $N_{1000\text{Hz}}$ trace to make a product of MV-FT (e.g. each foot of zone multiplied by $N_{1000\text{Hz}}$ amplitude). The MV-FT values are added for each zone and thus used to allocate the known surface production rate.

EXAMPLE 6

Example 6 shows the utility of this technique. The actual calculations are shown on the example. Zones A, B, and C are all members of a massive zone, which, in this case, has become fingered out updip. The lower portion of Zone B was not perforated because it was deemed unproductive due to a lack of permeability. Prior to production it was feared that the bottom zone would not be drained properly in view of the opened sections above (zones A & B). Results of the analysis are shown on the log. The bottom section is the best producer per unit foot of hole and is contributing about 50% of total production.

PART III - FLUID FLOW PAST THE SOUND LOGGER AS A NOISE SOURCE

- A. Single Phase Free Flow: The flow of a fluid past the sound logging sonde creates turbulence and, thus, radiates noise. In such a case the tool is equivalent to a flowmeter without moving parts. This condition is called a free-flow situation since the presence of the sonde in the flowing stream is the sound source. Once the tool is out of the flow stream, it no longer detects the flow noise. Incidentally, it is worthwhile to note that pipe turbulence is small compared to turbulence past the tool.

The logging sonde is sufficiently streamlined such that a respectable velocity past the tool is required to generate much noise. The low flow rate resolution is about that of commercial spinner-type flowmeters without packers. The 600Hz frequency cut is used as the reference signal. For sound created by flow past the tool the following proportionality is written:

$$N^*_{600\text{Hz}} \approx \Delta P \times q \quad (1)$$

This relates volumetric flow rate q , and the pressure drop ΔP across the tool. From fluid dynamics it is known that:

$$\Delta P = \frac{1}{2} C_D \rho V^2 \quad (2)$$

where: ρ = fluid density
 V = fluid velocity
 C_D = drag coefficient

Noting that velocity V is q divided by the sectional areas A_s , of cross-section between tool and pipe, the following relation can be written.

$$N^*_{600\text{Hz}} \approx C_D \rho \frac{q^2}{A_s^2} \times q \quad (3)$$

From this relation an "Audible Drag Coefficient", dependent only on Reynold's number, can be defined, viz:

$$\left\{ \begin{array}{l} C_D = \frac{2A_s^2 F_{f1} N^*_{600\text{Hz}}}{\rho q^3} \\ C_D = 4 \times 10^{-6} \text{ for turbulent flow} \end{array} \right. \quad (4)$$

where: $N^*_{600\text{Hz}}$ = log value 600Hz frequency cut corrected for cable losses (Figures 1 or 2).

A_s = $\frac{\pi}{4} (D_{\text{pipe}} + D_{\text{tool}})(D_{\text{pipe}} - D_{\text{tool}})$ cross sectional area for flow past tool, Sq. Ft. (Figure 7).

F_{f1} = fluid loading factor; 1 for liquid, 2 for gas

ρ = fluid density, #/cu. ft.

q = volumetric flow rate, thousands of cubic ft/day, (MCF/d) at downhole conditions.

The value for $C_D = 4 \times 10^{-6}$ was taken from Figure 8 which is an experimental correlation of C_D with Reynold's number for single phase flow. The value should be representative of most applications. The use of Equation 4 to calculate flow rates from noise levels is apparent, but it is necessary to insure that the measured noise, is, in fact, due to flow past the sonde and not residual noise from a nearby source.

- B. Two Phase Free Flow: The flow of gas-liquid mixtures past the tool creates a strong sound source in the 200-600Hz band due to the bubbling and slugging action of the gas as it "outruns" the liquid phase; a result of density difference of the phases.

Experimental tests have shown that for flowing gas-liquid volumetric ratios of 0.2 MCF/d or greater, a geometrical factor F_g for gas-liquid flow past the sonde can be defined such that the total volumetric flow rate can be determined by Equation 5:

$$q_t = \frac{\Delta^* F_g - 6}{9.1} \quad \text{for } q_t \geq 0.5 \text{ MCF/d}$$

$$\frac{q_{\text{gas}}}{q_{\text{liquid}}} \geq 0.20$$
(5)

where: $q_t = q_{\text{gas}} + q_{\text{liquid}}$, MCF/d

$\Delta^* = N^*_{200} - N^*_{600}$, log values of 200Hz and 600Hz corrected for cable losses (Figures 1 or 2).

If $F_g = 1$, then Eq. 5 is the equation of the straight line drawn in Figure 3, utilized in Part I. For very low total flow rates, Eq. 5 should be replaced by Eq. 6 below:

$$q_t = \frac{\Delta^* F_g}{31} ; \quad q_t < 0.5 \text{ MCF/d}$$
(6)

In the section on Well Geometrical Factor (Figures 1 and 2), a value of $F_g = 0.06$ is shown; this is, however, a composite value that attempts to include both oil-gas mixtures and water-gas mixtures up to moderate flow rates. For total flow rates up to 3-4 MCF/d, F_g is nearly independant of total flow velocity and is about constant at a value of 0.02 for gas-water mixtures and 0.080 for gas-oil mixtures. The larger F_g value is a consequence of the tendency of gas-oil mixtures to form foam that "cushions" the two phase activity. Values for the interfacial tension between gas-oil are only about one third those values for gas-water surface tensions; hence the greater tendency to foam. To a somewhat lesser extent the difference in F_g - values reflects the fact that the velocity of slippage (or buoyancy effect) for gas through oil is only about one third that for gas through water.

As the total flow rate increases, the gas and liquid phase tend to flow more together with a resultant decrease in two phase activity, Δ^* , and a corresponding increase in F_g as defined by Eq. 5. Figure 9 shows a correlation between F_g and, $q_t/A_s^{0.37}$:

$$F_g = f\left(\frac{q_t}{A_s^{0.37}}\right) \quad (7)$$

where: q_t = total flow rate, MCF/d

A_s = sectional area between tool and pipe, sq. ft.

The factor $A_s^{0.37}$ shows that F_g is a weak function of velocity as well as a stronger function of total flow rate. There are three curves on Figure 9; one each for gas-water, gas-oil, or gas-foamy water, and pure foam flow with the latter curve being only tentative. The data on Figure 9 covers the pipe sizes shown in the top left corner, flow rates from 0.10 MCF/d to 250 MCF/d, and gas-liquid flow rate ratios from 0.2 to 0.999. Actual values of gas volumetric hold up in the experiments ranged from 0.02 to 0.999. It is interesting to note that the noise logger does not "see" the discrete types of flow regimes that are supposed to exist in two-phase flow; that is, a smooth variation in F_g encompasses the bubble, slug, and froth regimes. Also, please note that at higher flow rates the gas-oil curve becomes coincident with the gas-water curve.

Exact use of Figure 9 would appear to be uncertain since the only known information is Δ^* and the type of fluids involved. If both sides of Eq. 5 are divided by $(A_s^{0.37})$, the resulting equation is:

$$\frac{q_t}{A_s^{0.37}} = \frac{\Delta^* F_g - 6}{9.1 A_s^{0.37}} \quad (8)$$

If, for a known value of Δ^* , and A_s , Eq. 8 is plotted on Figure 9, there will generally be two intersections with the appropriate F_g curve; one intersection at high flow rates and one at low flow rates. Thus the solution is nonunique in that it admits two solutions for each measured Δ^* value.

The uncertainty of Figure 9 can be partially resolved by use of Figure 10 which provides a first approximation to F_g by the use of a "Spectrum" test to distinguish between a high flow rate situation and a low flow rate situation. This is possible since the single phase, higher frequency noise levels increase as the two phase activity decreases. Thus the ratio,

$$\frac{N^* 2000}{\Delta^*}$$

is almost directly proportional to velocity. Figure 10 shows a correlation between F_g and the group shown:

$$F_g = f' \left(\frac{2A_s^{0.7} N^* 2000}{\Delta^*} \right) \quad (9)$$

This figure serves as an initial estimate of F_g to fix the approximate location on Figure 9. If only an estimate of flow rate is required, this value of F_g is good enough to use in Eq. 5. A closer estimate can usually be obtained by using the F_g value from Figure 10 in Eq. 8 to calculate one pair;

$$\left\{ F_g, \frac{q_t}{A_s^{0.37}} \right\}$$

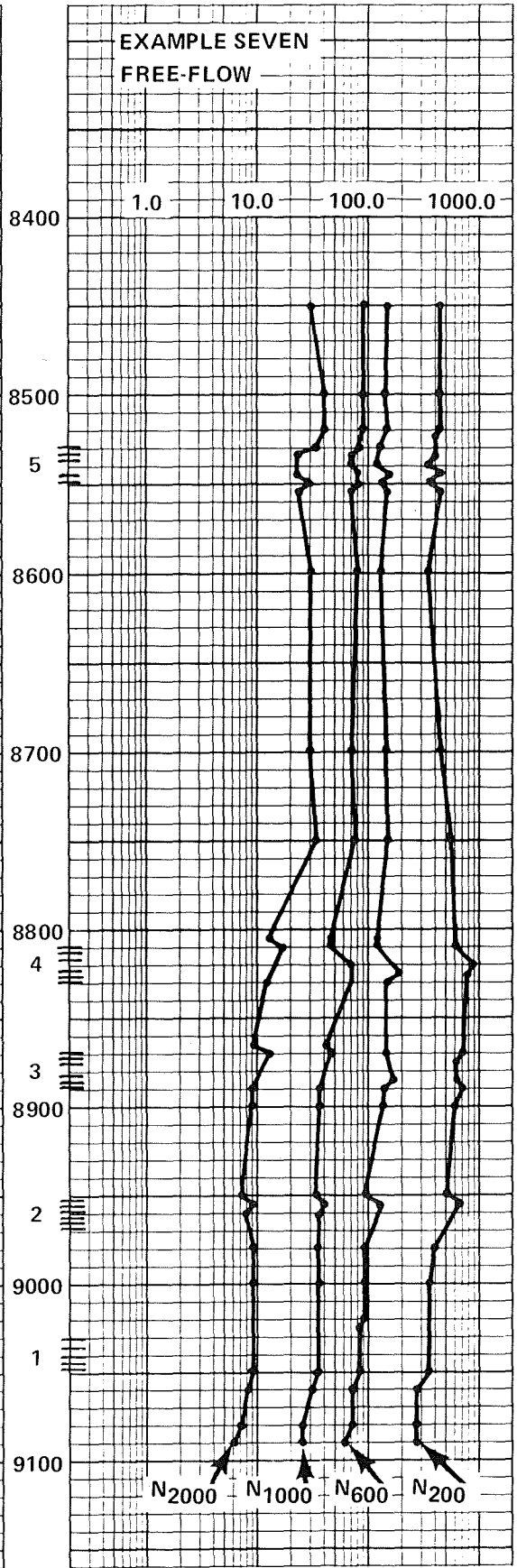
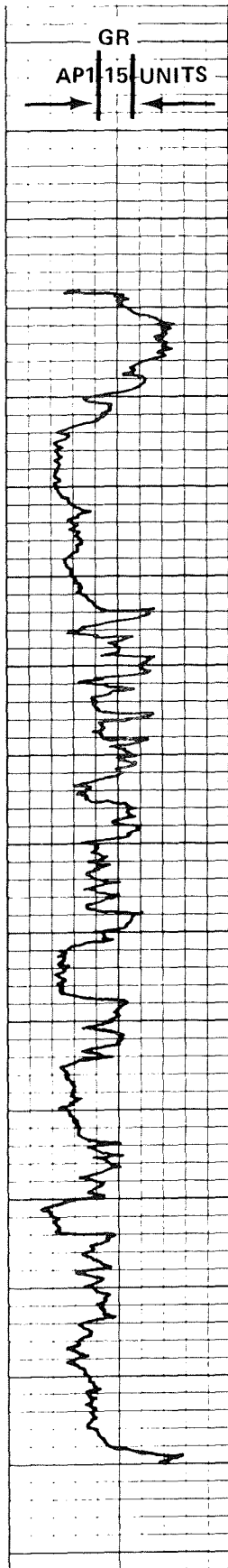
This pair is plotted on Figure 9; then Eq. 8 is used to calculate adjacent pairs and a line constructed to give the intersection with the appropriate curve on Figure 9. Once the intersection is established the total rate is then calculated from the ratio:

$$\frac{q_t}{A_s^{0.37}}$$

If only the gas phase is flowing, then Figure 10 over-estimates F_g and the corresponding construction on Figure 9 should be extended to find the low flow rate intersection even though this may require more than a two-fold change in F_g .

For low flowing ratios of gas to liquid ($\frac{q_{\text{gas}}}{q_{\text{liquid}}} = 0.10$) the above calculation procedure gives a total rate, q_t that is about equal to the actual gas rate q_{gas} , rather than the true total rate.

The best way to utilize correlations like Figures 9 & 10 is to measure a few correlation points in the field so that the curve appropriate to a particular type of environment can be sketched on the figures. This is particularly true for the foam flow line since the actual situation can be located at any point or locus of points between frothy liquid-gas to sure foam. Foam flow is much more common in field situations than would be suspected by study of published multiphase literature. Foam can be created at perforations where high velocities occur and then remain stable up the remainder of the wellbore. This is a point that can have serious implications in spinner interpretations since foam can have a considerably higher "viscosity" than even the liquid phase.



AT 8500', $N_{200} = 450$
 $N_{600} = 140$
 $N_{2000} = 40$
 $\Delta^* = 310$

AT 8650', $N_{200} = 400$
 $N_{600} = 130$
 $N_{2000} = 30$
 $\Delta^* = 270$

AT 8880', $N_{200} = 700$, $N_{600} = 140$
 $N_{2000} = 12$ $\Delta^* = 560$

AT 8900', $N_{200} = 600$, $N_{600} = 130$
 $N_{2000} = 9$ $\Delta^* = 470$

AT 9000', $N_{200} = 350$, $N_{600} = 90$,
 $N_{2000} = 9$ $\Delta^* = 260$

EXAMPLE 7

Example 7 is from a gas well that makes water in a somewhat peculiar manner. The well produces water-free for about three days and then dumps water. At the time of logging the well was flowing gas only at a rate of about 250 MSCF/d; it is therefore likely that only the gas phase is moving downhole.

Casing is 5 1/2", tubing is 2 1/2" with packer set at 8443'. Flowing surface pressure is 250 psi. Survey conducted on 20,000' of 5/16" cable.

Starting at the bottom set of perforations (1) two phase activity, as determined by Δ^* , increases in the wellbore progressing upward to the middle of perforations set (4) where the two phase activity decreases and the 2000Hz level increases. Apparently at this point, a sufficient volumetric gas rate is entering the wellbore at this location to create a frothy water flow condition. It also appears that there is a sort of "liquid level" standing at about 8820' at the middle of the fourth set of perforations. It appears that the water source is at or below this depth.

The two phase flow chart (Figure 10) will be used with log readings taken above each set of perforations to establish a productivity profile. Below 8820', the gas-water lines of Figures 9 & 10 are appropriate, while above this depth, the foamy water-gas curves will be used. Since only the gas phase is moving, Figure 10 will likely over-estimate F_g and thus production rate.

Log values above each zone are tabulated on Example 7. Since the cable correction factor (CF) for $N_{600\text{Hz}}$ is very small, it will be ignored. The N_{2000} values from the log must be multiplied by 1.35 before entering the chart. For this particular weight of 5 1/2" pipe, $A_s = 0.1164$. Accordingly corrected values, ratios and F_g estimates are as follows:

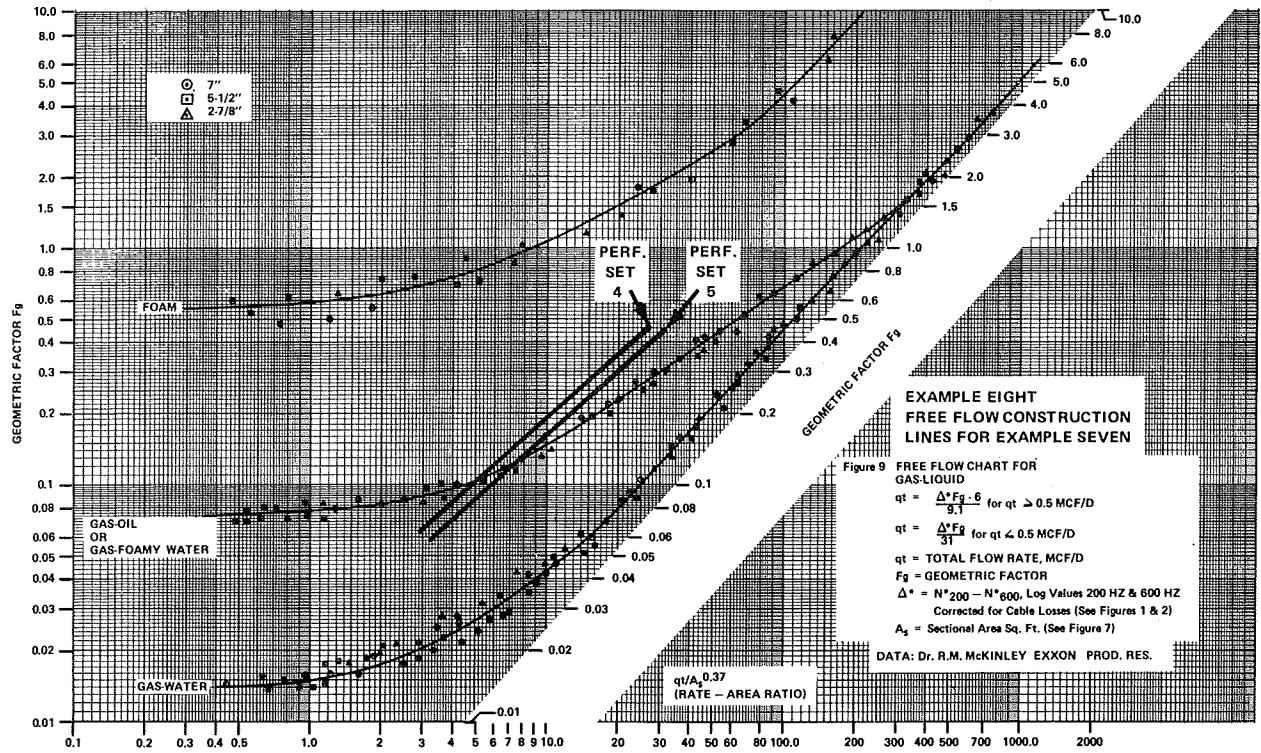
Above Perf. Set #	N^*_{200}	N^*_{600}	N_{2000}	N^*_{2000}	*	$\frac{2A_s^{0.7} N^*_{2000}}{\Delta^*}$	F_g	Type Flow
1	350	90	9	12.2	260	0.020	0.02	Gas-Water
2	600	130	9	12.2	470	0.011	0.015	Gas-Water
3	700	140	12	16.2	560	0.013	0.015	Gas-Water
4	400	130	30	40.5	270	0.066	0.44	Gas-Foamy Water
5	450	140	40	54	310	0.077	0.48	Gas-Foamy Water

From Figure 10 it can be assumed that $F_g = 0.015$ for perforation sets 1, 2, and 3, and this value is relatively flow independent, and equal to 0.015. Zones 4 and 5 are apparently foam flow and, as first estimates, will be treated as such. The construction equation to be plotted on Figure 9 is:

$$\frac{q_t}{A_s^{0.37}} = \frac{\Delta^* F_g - 6}{(0.4512)(9.1)} = \frac{\Delta^* F_g - 6}{4.11} \quad (10)$$

Computed pairs for perforation sets 4 and 5 are:

Perf. Set.	Est. F_g	q_t/A_s
4	0.44	27.4
4	0.10	5.1
5	0.48	34.7
5	0.10	6.1

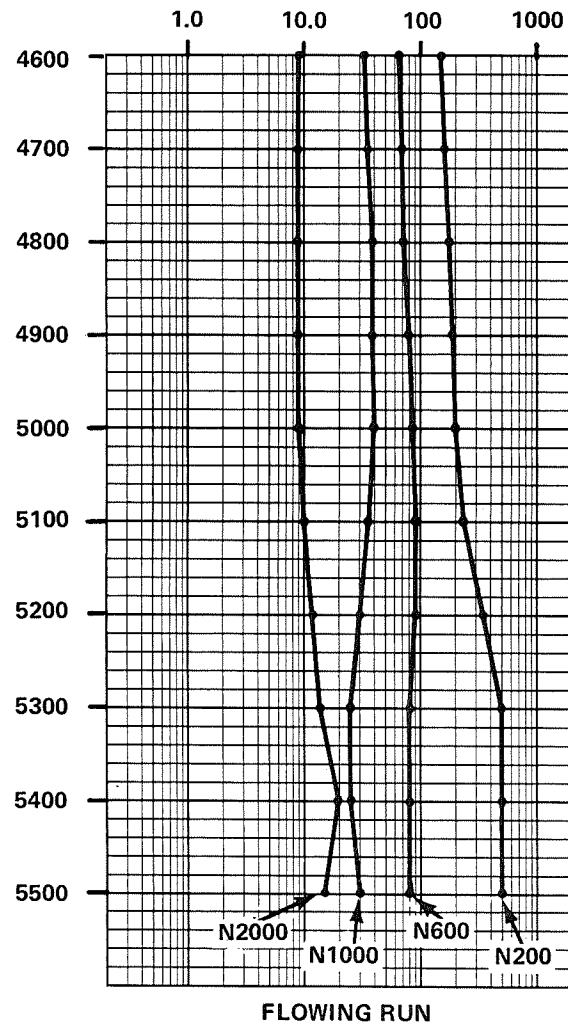
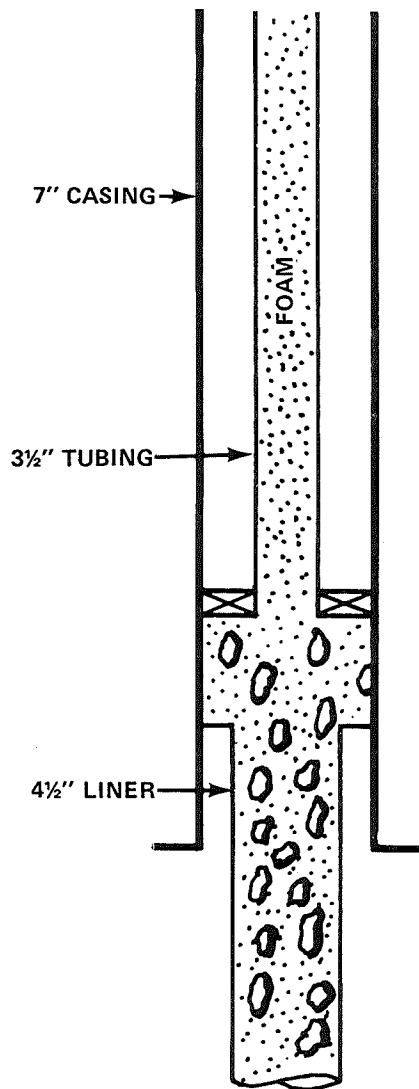


EXAMPLE 8

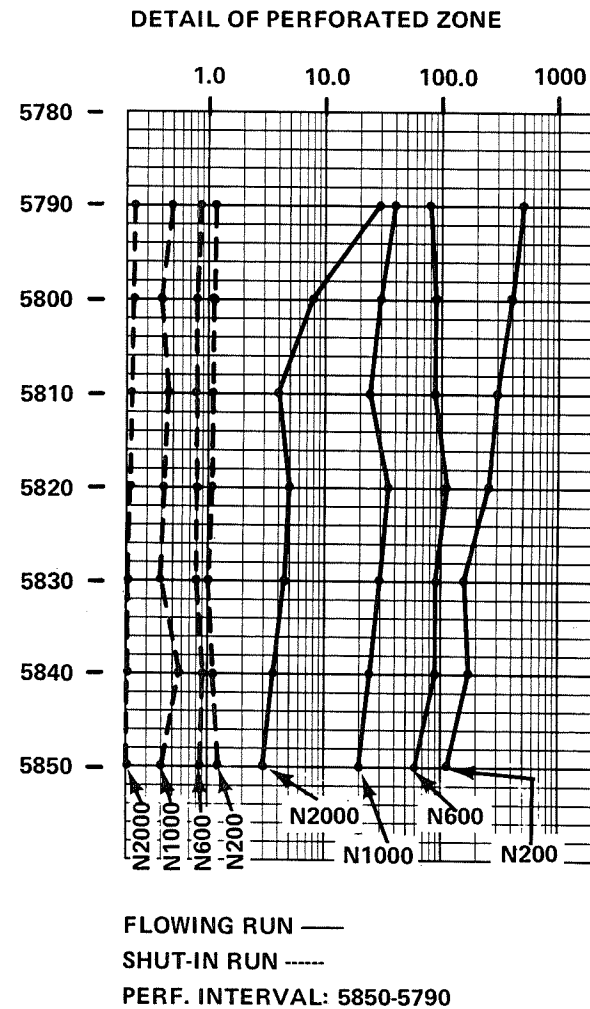
These two sets are plotted as shown on Example 8 and the corrected values of F_g are determined. Calculations of flow above each zone is shown below:

Above Perf. Set	F_g	Δ^*	$q_t = \frac{\Delta^* F_g - 6}{9.1}$	or	$q_t = \frac{\Delta^* F_g}{31}$
1	0.015	260	0.13		MCF/d
2	0.015	470	0.23		MCF/d
3	0.015	560	0.27		MCF/d
4	0.11	270	2.60		MCF/d
5	0.135	310	3.94		MCF/d

Use $q_t = \frac{\Delta^* F_g}{31}$ for flow rates less than 0.5 MCF.



EXAMPLE NINE
GAS - OIL FREE FLOW



Perforation sets 4 and 5 are obviously contributing most of the gas production. A thru-tubing bridge plug was set below perforation set 4; gas production remained essentially unchanged and water production dropped to essentially zero.

With BHT estimated at 250°F and BHP estimated to be 1350 psi (250 psi flowing surface pressure), the volume correction factor (Sp.Gr. 0.8) from Figure 6 is 74.

$$q_{std} = (3.94 \text{ MCF/d})(74) = 291 \text{ MSCF/d}$$

Measured surface flow rate is 250 MSCF/d. This shows reasonable agreement between (within 20%) calculated and actual flow rates. The technique used in Example 7 can also be used to determine the flow profile of moderate and low flow rate gas wells. The flow above each perforation set is computed and the difference provides an index of total flow.

EXAMPLE 9

Example 9 is an oil completion in a gas-cap reservoir where gas is injected for pressure maintenance. The well was surveyed to determine the cause of an overly high GOR. Flow rate is 2100 bbls/d with 1.2 MMCF/d gas in excess of lift gas. Reservoir GOR is 350 SCF/bbl while production GOR is 500 SCF/bbl. Obviously, injected gas is being wasted in excess GOR.

The well was shut-in and logged with results shown as the dashed lines on Perforation Detail portion of Example 9. Since all sound levels are quite low it was concluded that no gas was moving into the perforated interval from other zones.

The perforated zone was logged while producing; the solid traces on the Perforation Detail show the results. Note that both $N_{1000\text{Hz}}$ and $N_{2000\text{Hz}}$ values increase at 5810'; this is the source of excess gas and is caused by coning downward during routine production operations. Note also at the base of the perforated zone that the $N_{200\text{Hz}}$ and $N_{600\text{Hz}}$ traces are quite close together indicating single phase flow while at the top of zone these two curves are widely separated indicating that the flow has changed to two-phase gas-liquid.

Two flow situations (e.g. 4 1/2" liner and 3 1/2" tubing) will now be analyzed as free flow situations.

4 1/2" Liner: From Figure 7, $A_s = 0.0717$, $A_s^{0.7} = 0.1581$, $A_s^{0.37} = 0.3772$.

Log values (at 5300') corrected for cable losses are:

$$\Delta^* = 420\text{MV}, N^*_{2000\text{Hz}} = 28.9\text{MV}$$

The spectrum ratio is:

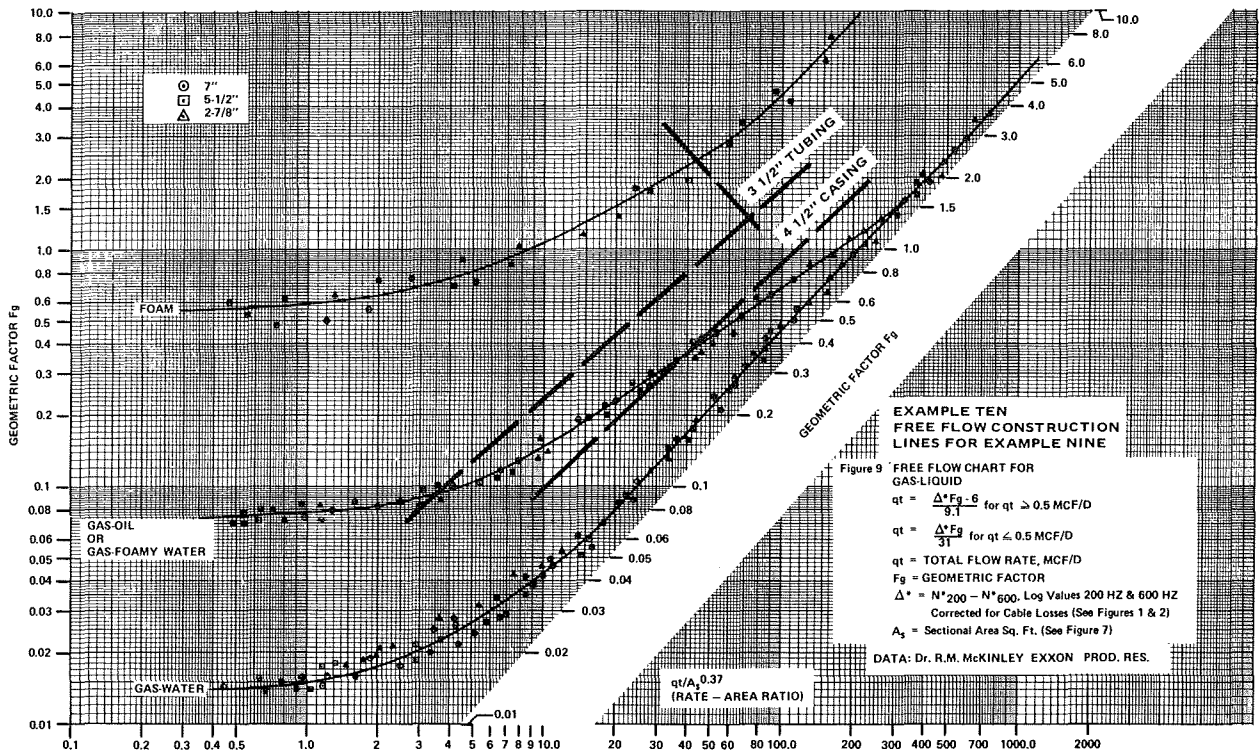
$$\frac{(2)(0.1581)(28.9)}{(42)} = 0.022$$

From the gas-oil correlation of Figure 10, $F_g = 0.175$; using the construction equation:

$$q_t/A_s^{0.37} = \frac{\Delta^* F_g - 6}{(0.3772)(9.1)}$$

the following pairs were computed:

F_g	$q_t/A_s^{0.37}$
0.175	19.6
1.0	120.6



EXAMPLE 10

Plotting this line as shown on Example 10 (marked 4 1/2" casing),

$$F_g = 0.42 \text{ and } q_t/A_s^{0.37} = 50; q_t = (50)(0.3772) = 18.8 \text{ MCF/d}$$

Known surface flow rate of 2100 bbls/d can be converted to 2100/0.178 equals 11.8 MCF/d gas flow.

Thus the free or excess gas (at reservoir conditions) being made by this well is:

$$18.8 - 11.8 = 7 \text{ MCF/d.}$$

Estimates of reservoir temperature (150°F) and pressure (2000 psi) give a

volume correction factor of 155. Accordingly the excess gas converted to standard conditions is:

$$q_{\text{excess}} = (7 \text{ MCF/d})(155) = 1.1 \text{ MMSCF/d}$$

This is in reasonable agreement with the surface measured 1.2 MMSCF/d.

3 1/2" Tubing: Entry of production into the 3 1/2" tubing should produce an increase in sound levels since the same mass flow rate is flowing through a smaller surface area; such is not the case. Apparently, the higher velocity of flow in the tubing has caused the flow to convert from gas-oil to foam.

Sound levels, F_g levels, etc., are tabulated below:

Depth	Δ^*	$N^*_{2000\text{Hz}}$	$\frac{2A_s^{0.7} N^*_{2000\text{Hz}}}{\Delta^*}$	F_g (foam)	$q_t/A_s^{0.37}$
5100	150	17	0.021	1.5	84.7
5000	115	17	0.027	1.6	68.8
4900	100	15.3	0.028	1.6	63.5
4800	100	15.3	0.028	1.6	63.5

Plotting these points on the rate-area ratio graph (Example 10) it can be observed that these points form a progression towards the foam line with decreasing well depth. The construction equation is computed in the usual manner and plotted on Example 10. Next, a perpendicular to the construction equation through the shallowest depth point is made and extended to intersect the foam flow curve,

$$(F_g = 2.4, q_t/A_s^{0.37} = 45).$$

Flow rate is:

$$q_t = (0.284)(45) = 12.8 \text{ MCF/d.}$$

This is in reasonable agreement (11.8 MCF/d at the surface) since the foam flow curve is tentative, and will be refined with subsequent experience.

The sound levels produced by foam have all of the characteristics of single phase flow, since no slugging exists to generate low frequency energy. All sound levels in foam flow are higher than what would be expected for an equivalent single phase flow rate. When flow conditions are such that foam can be generated (e.g. high gas velocity at perforations) it is always prudent to make a calculation check of flow rate assuming both single phase and foam flow, and compare these rates to known data.

CONCLUSION

The sound logging device is a useful addition to the present array of production logging tools. By the nature of its measurement it will find wide use, both as a single tool, and as part of complimentary suites of production logs used to guide remedial workover programs.

E. L. (Lee) Britt is Training Supervisor for GO International, Inc. in Fort Worth.

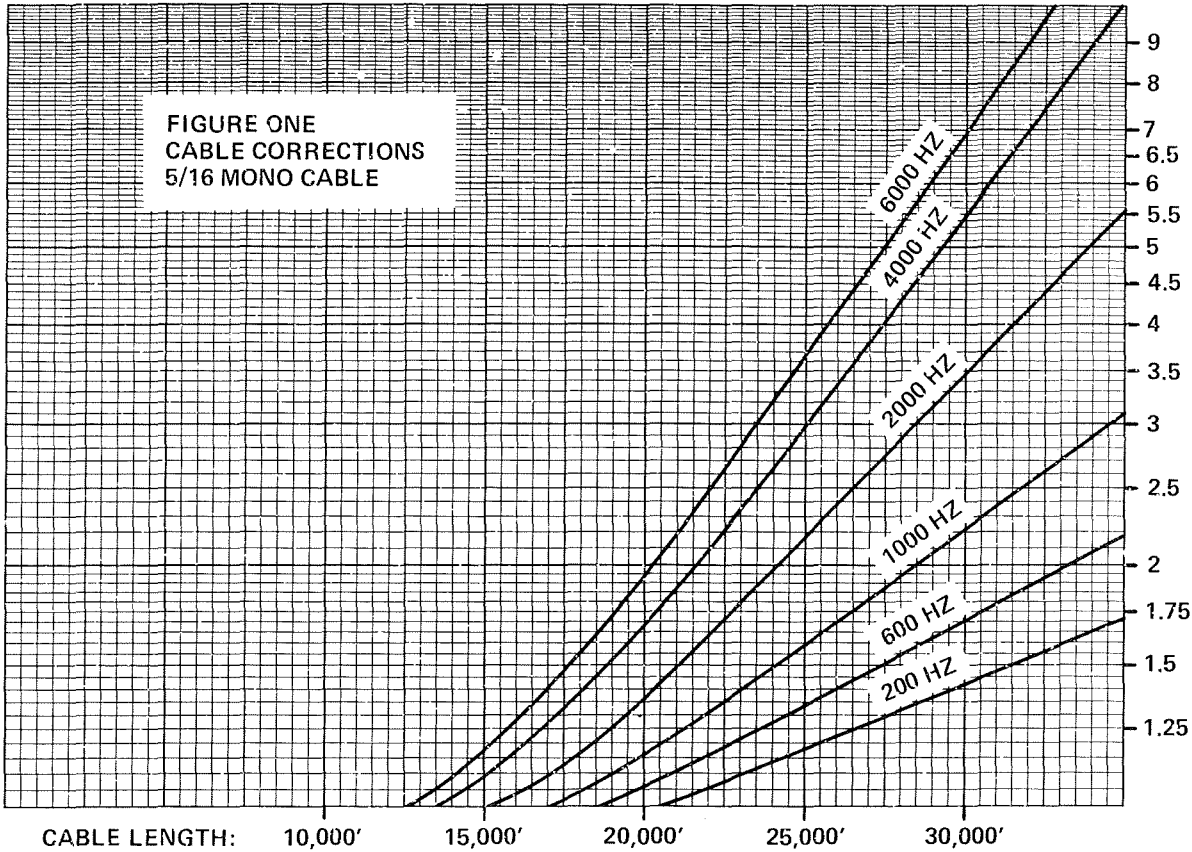


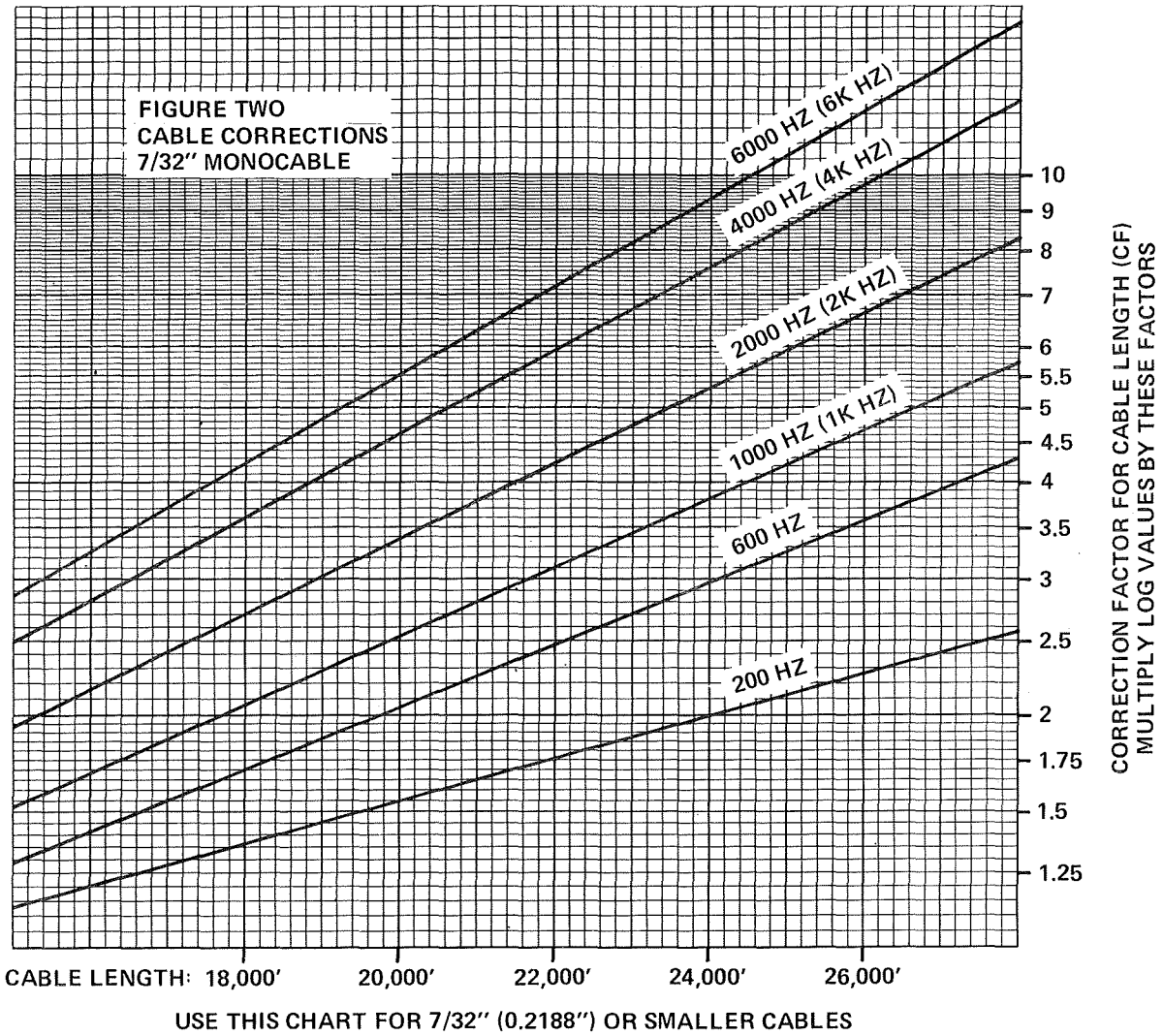
FIGURE ONE
CABLE CORRECTIONS
5/16 MONO CABLE

CORRECTION FACTOR FOR CABLE LENGTH (CF)
MULTIPLY LOG VALUES BY THESE FACTORS

CABLE LENGTH: 10,000' 15,000' 20,000' 25,000' 30,000'

USE THIS CHART FOR 5/16" (0.3125") OR LARGER CABLES

WELL GEOMETRY FACTOR (Fg)			EXAMPLE OF CORRECTIONS		
TYPE OF WELL	FLUID CONTENT	FACTOR			
Tubingless Completion	Liquid	1.0	Tubing String in Casing with liquid in Tubing and Annulus; Log readings are: 200 Hz - 125 MV; 600 HZ - 70 MV; 1000 HZ - 10 MV; 2000 HZ - 3 MV CABLE: 25,000' of 5/16" line		
	Gas	1.0 - 2.0			
Tubing String In Casing	Tubing: Liquid	2.0		$N_{200}^* = (125 \text{ MV}) (1.17) = 146.25 \text{ MV}$	
	Annulus: Liquid			$N_{600}^* = (70 \text{ MV}) (1.34) = \underline{93.8 \text{ MV}}$ $\Delta^* = 52.45 \text{ MV}$	
Tubing String In Casing	Tubing: Gas	2.0 - 4.0		$N_{1000}^* = (10 \text{ MV}) (1.59) = 15.9 \text{ MV}$	
	Annulus: Liquid Or Vice Versa			$N_{2000}^* = (3 \text{ MV}) (2.15) = 6.5 \text{ MV}$	
Tubing String In Casing	Tubing: Gas Annulus: Gas	5.0 - 10.0			
Leak Into Same String As Detector - Tubing or Casing	Two Phase, Gas - Liquid Leak	0.06			
	Single Phase Leak	0.20			



WELL GEOMETRY FACTOR (Fg)		
TYPE OF WELL	FLUID CONTENT	FACTOR
Tubingless Completion	Liquid	1.0
	Gas	1.0 - 2.0
Tubing String In Casing	Tubing: Liquid	2.0
	Annulus: Liquid	
Tubing String In Casing	Tubing: Gas	2.0 - 4.0
	Annulus: Liquid Or Vice Versa	
Tubing String In Casing	Tubing: Gas Annulus: Gas	5.0 - 10.0
Leak Into Same String As Detector - Tubing or Casing	Two Phase, Gas - Liquid Leak	0.06
	Single Phase Leak	0.20

EXAMPLE OF CORRECTIONS
Leak Into Same String Two Phase (Tubingless Completion): Log Readings Are: 200 Hz - 600 MV; 600 HZ - 200 MV; 1000 HZ - 100 MV; 2000 HZ - 25 MV; CABLE: 20,000 of 7/32" line
$N_{200}^* = (600\text{MV}) \left(\frac{\text{CF}}{1.54} \right) = 924\text{MV}$
$N_{600}^* = (200\text{MV}) \left(\frac{\text{CF}}{2.02} \right) = 404\text{MV}$ $\Delta^* = 520\text{MV}$
$N_{1000}^* = (100\text{MV}) \left(\frac{\text{CF}}{2.5} \right) = 250\text{MV}$
$N_{2000}^* = (25\text{MV}) \left(\frac{\text{CF}}{3.35} \right) = 83.8\text{MV}$

**FIGURE THREE
NOISE VS FLOW RATE FOR FLOW
OUTSIDE OF CASING
(TWO PHASE: GAS-LIQUID)**

$\Delta^* F_g = N^*200 - N^*600$; N^*200 and N^*600
Are Log Values Corrected for Cable Factor

F_g is Well Geometrical Factor

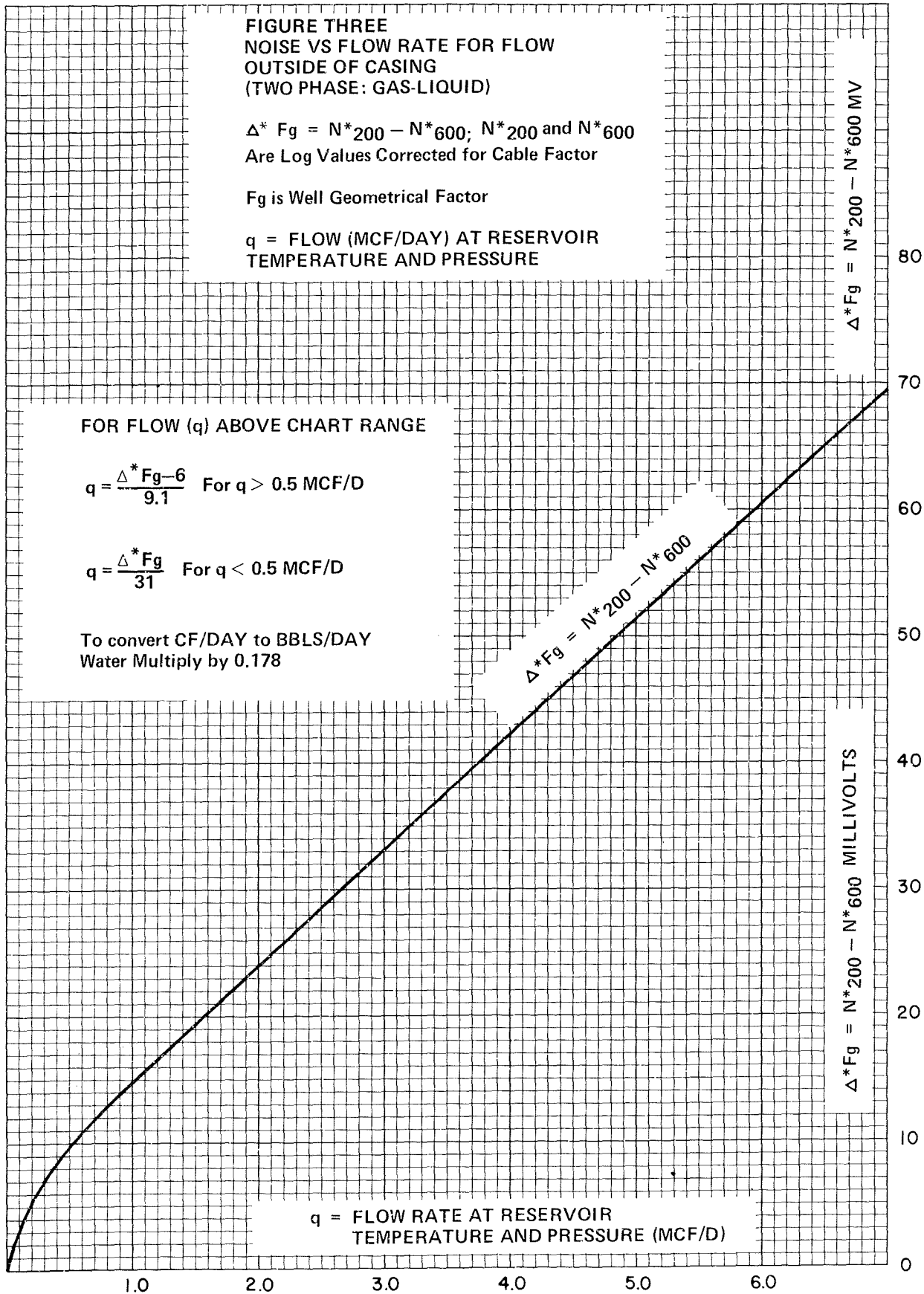
q = FLOW (MCF/DAY) AT RESERVOIR
TEMPERATURE AND PRESSURE

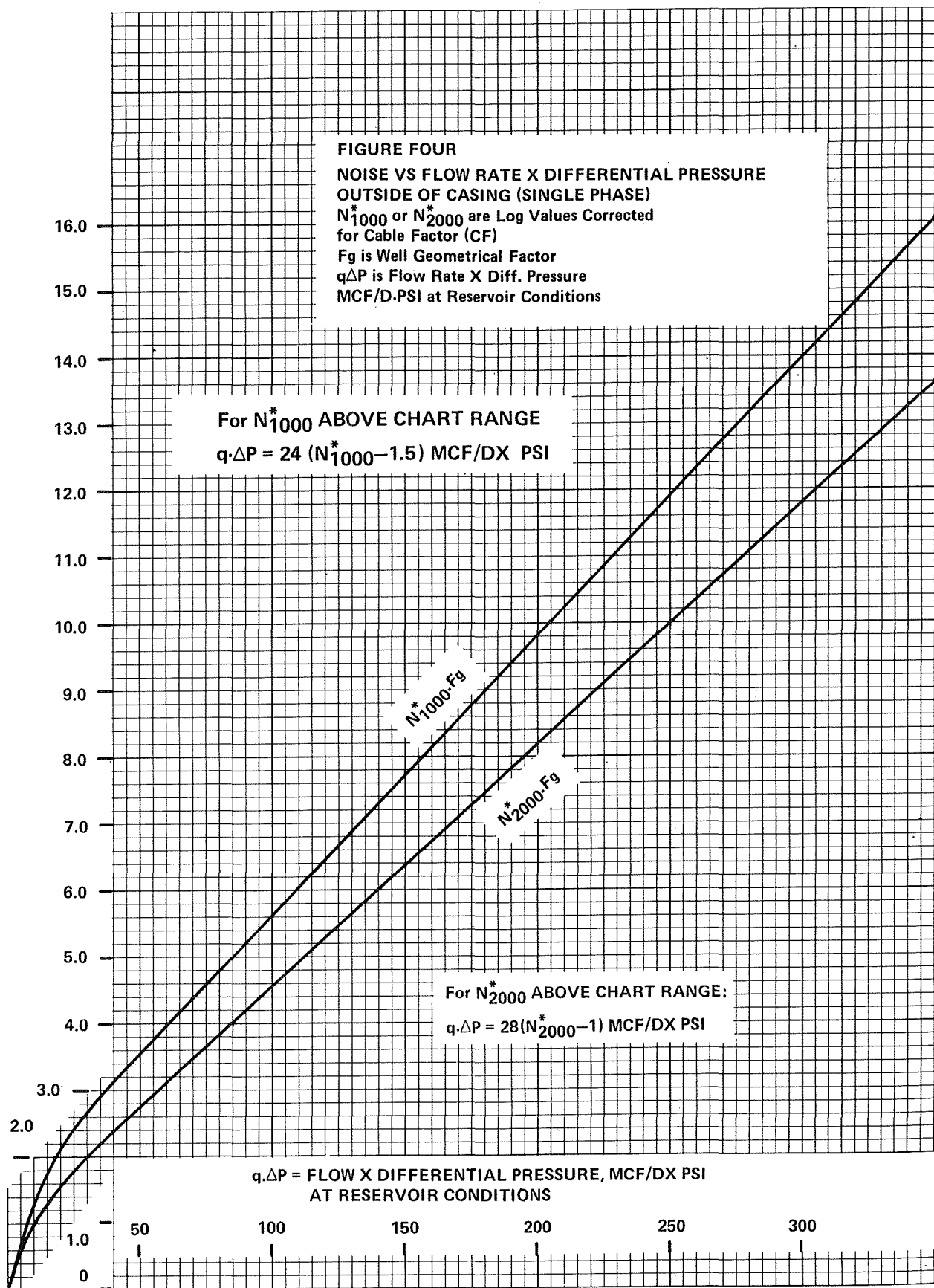
FOR FLOW (q) ABOVE CHART RANGE

$$q = \frac{\Delta^* F_g - 6}{9.1} \quad \text{For } q > 0.5 \text{ MCF/D}$$

$$q = \frac{\Delta^* F_g}{31} \quad \text{For } q < 0.5 \text{ MCF/D}$$

To convert CF/DAY to BBLS/DAY
Water Multiply by 0.178





**FLOW RATE VOLUME CONVERSION from
RESERVOIR CONDITIONS to
STANDARD CONDITIONS of
14.69 PSI. and 60°F (520° R)**

DATA: NGPSA
NATURAL GAS — MOL. WT. 17.40
Sp. Gr. 0.6 $P_c = 672$ PSI; $T_c = 380^\circ R$

GAS DENSITY (ENGLISH UNITS)
AT P.T. = (VOLUME FACTOR AT P.T.)
(0.0458) #/cu. ft.

GAS DENSITY (METRIC UNITS)
= (DENS. #/cu. ft.)
(0.01603)

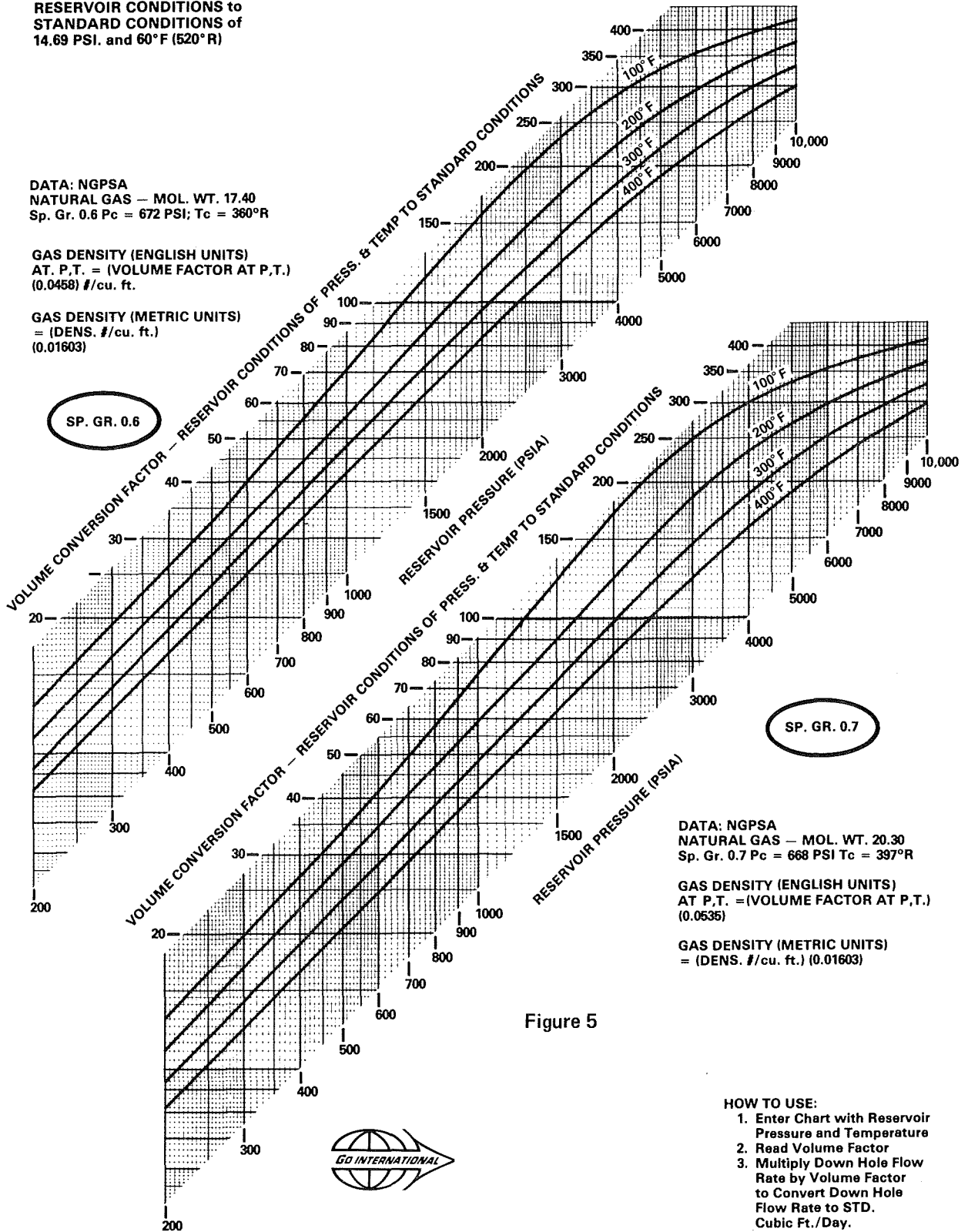


Figure 5



HOW TO USE:

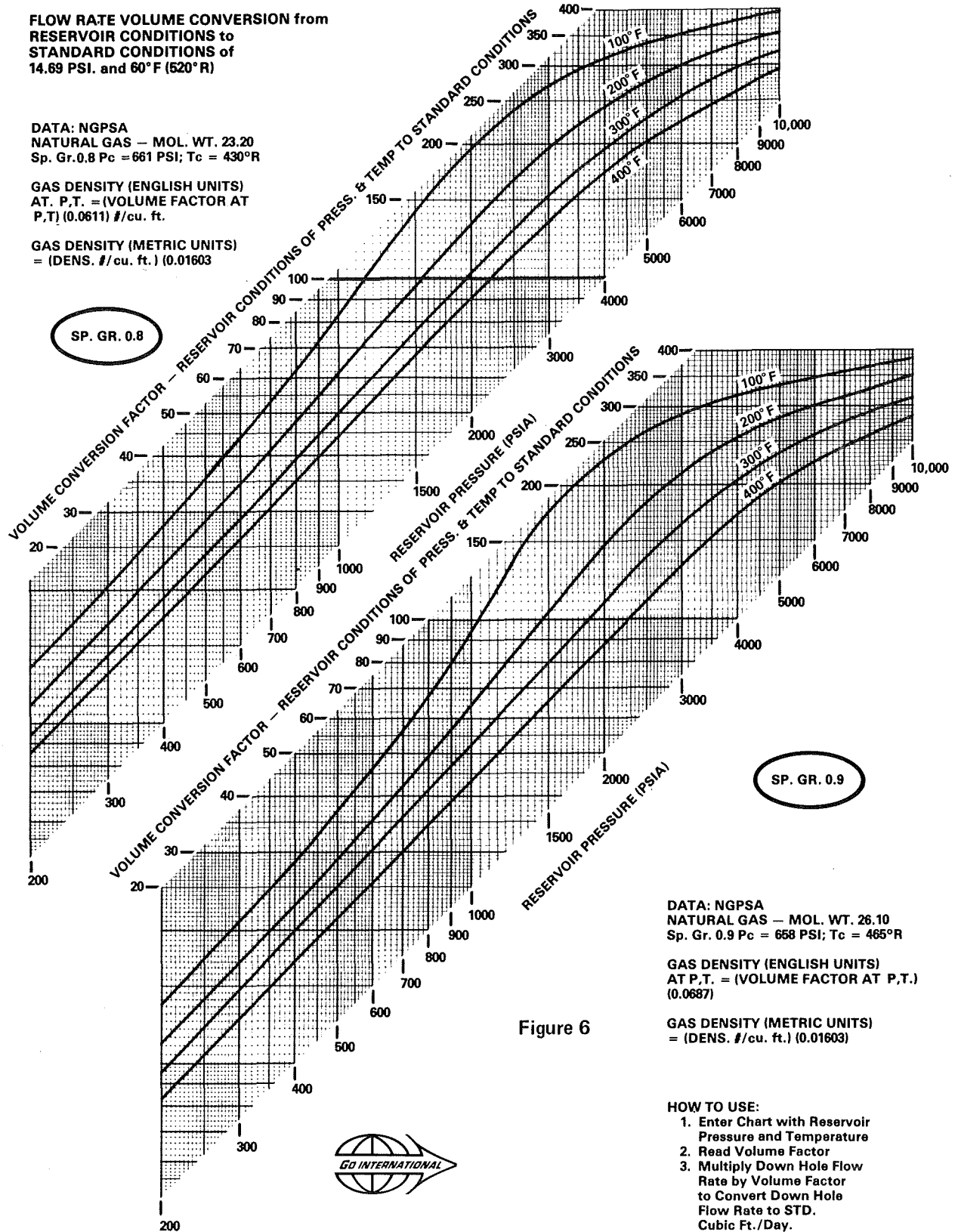
1. Enter Chart with Reservoir Pressure and Temperature
2. Read Volume Factor
3. Multiply Down Hole Flow Rate by Volume Factor to Convert Down Hole Flow Rate to STD. Cubic Ft./Day.

**FLOW RATE VOLUME CONVERSION from
RESERVOIR CONDITIONS to
STANDARD CONDITIONS of
14.69 PSI. and 60° F (520° R)**

DATA: NGPSA
NATURAL GAS — MOL. WT. 23.20
Sp. Gr. 0.8 $P_c = 661$ PSI; $T_c = 430^\circ R$

GAS DENSITY (ENGLISH UNITS)
AT P.T. = (VOLUME FACTOR AT
P.T.) (0.0611) #/cu. ft.

GAS DENSITY (METRIC UNITS)
= (DENS. #/cu. ft.) (0.01603)



SP. GR. 0.8

SP. GR. 0.9

DATA: NGPSA
NATURAL GAS — MOL. WT. 26.10
Sp. Gr. 0.9 $P_c = 658$ PSI; $T_c = 465^\circ R$

GAS DENSITY (ENGLISH UNITS)
AT P.T. = (VOLUME FACTOR AT P.T.)
(0.0687)

GAS DENSITY (METRIC UNITS)
= (DENS. #/cu. ft.) (0.01603)

Figure 6

HOW TO USE:

1. Enter Chart with Reservoir Pressure and Temperature
2. Read Volume Factor
3. Multiply Down Hole Flow Rate by Volume Factor to Convert Down Hole Flow Rate to STD. Cubic Ft./Day.



FIGURE SEVEN

$$A_s = \frac{\pi}{4} (D_{\text{pipe}} - D_{\text{tool}}) (D_{\text{pipe}} + D_{\text{tool}}) \text{ Sq. Ft.} \quad D_{\text{tool}} = 1.6875''$$

Size O.D.	Weight #/Ft.	I.D. Inches	A_s	A_s^2	$A_s^{0.7}$	$A_s^{0.37}$	D_e
2 3/8	4.70	1.995	0.0062	$4 \cdot 10^{-5}$	0.0285	0.1525	0.0256
	5.95	1.867	0.0035	$1 \cdot 10^{-5}$	0.0191	0.1234	0.0150
2 7/8	6.50	2.441	0.0170	0.0003	0.0577	0.2214	0.0628
	8.70	2.259	0.0123	0.0002	0.0460	0.1966	0.0476
3 1/2	9.30	2.992	0.0333	0.0011	0.0924	0.2840	0.1087
	12.95	2.750	0.0257	0.0006	0.0771	0.2580	0.0885
4	11.00	3.476	0.0504	0.0025	0.1235	0.3311	0.1490
4 1/2	9.50	4.090	0.0757	0.0057	0.1642	0.3848	0.2002
	10.50	4.052	0.0740	0.0055	0.1616	0.3816	0.1970
	11.60	4.000	0.0717	0.0051	0.1581	0.3772	0.1927
	12.75	3.958	0.0694	0.0048	0.1545	0.3727	0.1892
	13.50	3.920	0.0683	0.0047	0.1528	0.3705	0.1860
	15.10	3.826	0.0643	0.0041	0.1465	0.3623	0.1782
5	11.50	4.560	0.0979	0.0096	0.1966	0.4232	0.2394
	13.00	4.494	0.0946	0.0089	0.1919	0.4179	0.2339
	15.00	4.408	0.0904	0.0082	0.1859	0.4109	0.2267
	18.00	4.276	0.0842	0.0071	0.1769	0.4003	0.2157
5 1/2	13.00	4.919	0.1164	0.0135	0.2219	0.4512	0.2693
	14.00	4.887	0.1147	0.0132	0.2196	0.4488	0.2666
	15.50	4.825	0.1114	0.0124	0.2152	0.4440	0.2615
	17.00	4.767	0.1084	0.0118	0.2111	0.4395	0.2566
	20.00	4.653	0.1026	0.0105	0.2031	0.4307	0.2471
	23.00	4.545	0.0971	0.0094	0.1955	0.4220	0.2381
6	15.00	5.524	0.1509	0.0228	0.2661	0.4967	0.3197
	18.00	5.424	0.1449	0.0210	0.2587	0.4893	0.3114
	20.00	5.352	0.1407	0.0198	0.2534	0.4840	0.3054
	23.00	5.240	0.1342	0.0180	0.2451	0.4756	0.2960
	26.00	5.132	0.1281	0.0164	0.2373	0.4675	0.2870
6 5/8	17.00	6.135	0.1898	0.0360	0.3125	0.5407	0.3706
	20.00	6.049	0.1840	0.0339	0.3058	0.5345	0.3635
	24.00	5.796	0.1677	0.0281	0.2865	0.5165	0.3424
	28.00	5.666	0.1596	0.0255	0.2768	0.5071	0.3315
	32.00	5.550	0.1549	0.0240	0.2710	0.5016	0.3219
7	17.00	6.538	0.2176	0.0473	0.3438	0.5688	0.4042
	20.00	6.456	0.2118	0.0449	0.3374	0.5631	0.3974
	23.00	6.366	0.2055	0.0422	0.3303	0.5569	0.3899
	26.00	6.276	0.1993	0.0397	0.3233	0.5506	0.3824
	29.00	6.184	0.1930	0.0372	0.3161	0.5441	0.3774
	32.00	6.094	0.1870	0.0350	0.3092	0.5378	0.3672
	35.00	5.879	0.1730	0.0299	0.2928	0.5225	0.3493
	38.00	5.795	0.1676	0.0281	0.2864	0.5164	0.3423
7 5/8	20.00	7.125	0.2614	0.0683	0.3909	0.6087	0.4531
	24.00	7.025	0.2536	0.0643	0.3827	0.6019	0.4448
	26.40	6.969	0.2494	0.0622	0.3783	0.5982	0.4401
	29.70	6.875	0.2423	0.0587	0.3707	0.5918	0.4323
	33.70	6.765	0.2341	0.0548	0.3619	0.5844	0.4231
	39.00	6.625	0.2239	0.0501	0.3508	0.5748	0.4115

FIGURE SEVEN (Continued)

Size O.D.	Weight #/Ft.	I.D. Inches	As	As ²	As ^{0.7}	As ^{0.37}	De
8 5/8	24.00	8.097	0.3421	0.1170	0.4720	0.6724	0.5341
	28.00	8.017	0.3350	0.1122	0.4651	0.6672	0.5275
	32.00	7.921	0.3267	0.1067	0.4570	0.6611	0.5195
	36.00	7.825	0.3184	0.1014	0.4488	0.6548	0.5115
	40.00	7.725	0.3099	0.0960	0.4404	0.6483	0.5031
	44.00	7.625	0.3016	0.0910	0.4321	0.6418	0.4948
	49.00	7.511	0.2922	0.0854	0.4226	0.6343	0.4853
9 5/8	29.30	9.063	0.4325	0.1871	0.5561	0.7334	0.6146
	32.30	9.001	0.4264	0.1818	0.5506	0.7295	0.6095
	36.00	8.921	0.4185	0.1751	0.5435	0.7245	0.6028
	40.00	8.835	0.4102	0.1683	0.5359	0.7191	0.5956
	43.50	8.755	0.4025	0.1620	0.5289	0.7141	0.5890
	47.00	8.681	0.3955	0.1564	0.5224	0.7095	0.5828
	53.50	8.535	0.3818	0.1458	0.5097	0.7003	0.5706
10 3/4	32.75	10.192	0.5510	0.3036	0.6589	0.8021	0.7087
	40.50	10.050	0.5354	0.2867	0.6458	0.7936	0.6969
	45.50	9.950	0.5254	0.2760	0.6373	0.7881	0.6885
	51.00	9.850	0.5136	0.2638	0.6272	0.7815	0.6802
	55.50	9.760	0.5040	0.2540	0.6190	0.7761	0.6727
	60.70	9.660	0.4934	0.2434	0.6099	0.7700	0.6644
	65.70	9.560	0.4829	0.2332	0.6008	0.7639	0.6560
11 3/4	38.00	11.150	0.6625	0.4389	0.7496	0.8587	0.7885
	42.00	11.084	0.6545	0.4284	0.7433	0.8548	0.7830
	47.00	11.000	0.6444	0.4153	0.7352	0.8499	0.7760
	54.00	10.880	0.6301	0.3970	0.7237	0.8429	0.7660
	60.00	10.772	0.6173	0.3811	0.7134	0.8365	0.7570
13 3/8	48.00	12.715	0.8662	0.7503	0.9043	0.9482	0.9190
	54.50	12.615	0.8524	0.7266	0.8942	0.9426	0.9106
	61.00	12.515	0.8387	0.7034	0.8841	0.9370	0.9023
	68.00	12.415	0.8251	0.6808	0.8741	0.9313	0.8940
	72.00	12.347	0.8159	0.6657	0.8673	0.9275	0.8883

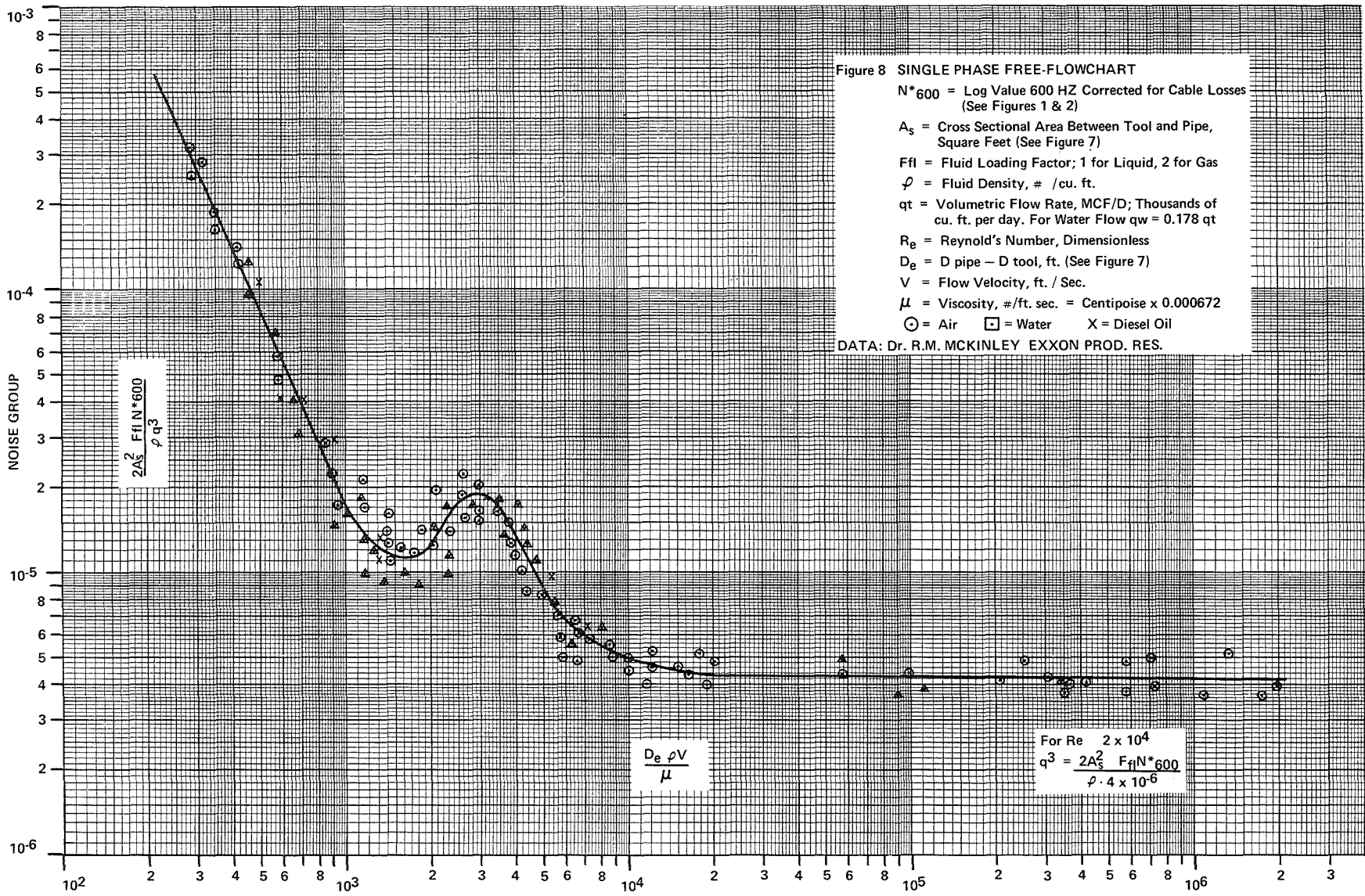
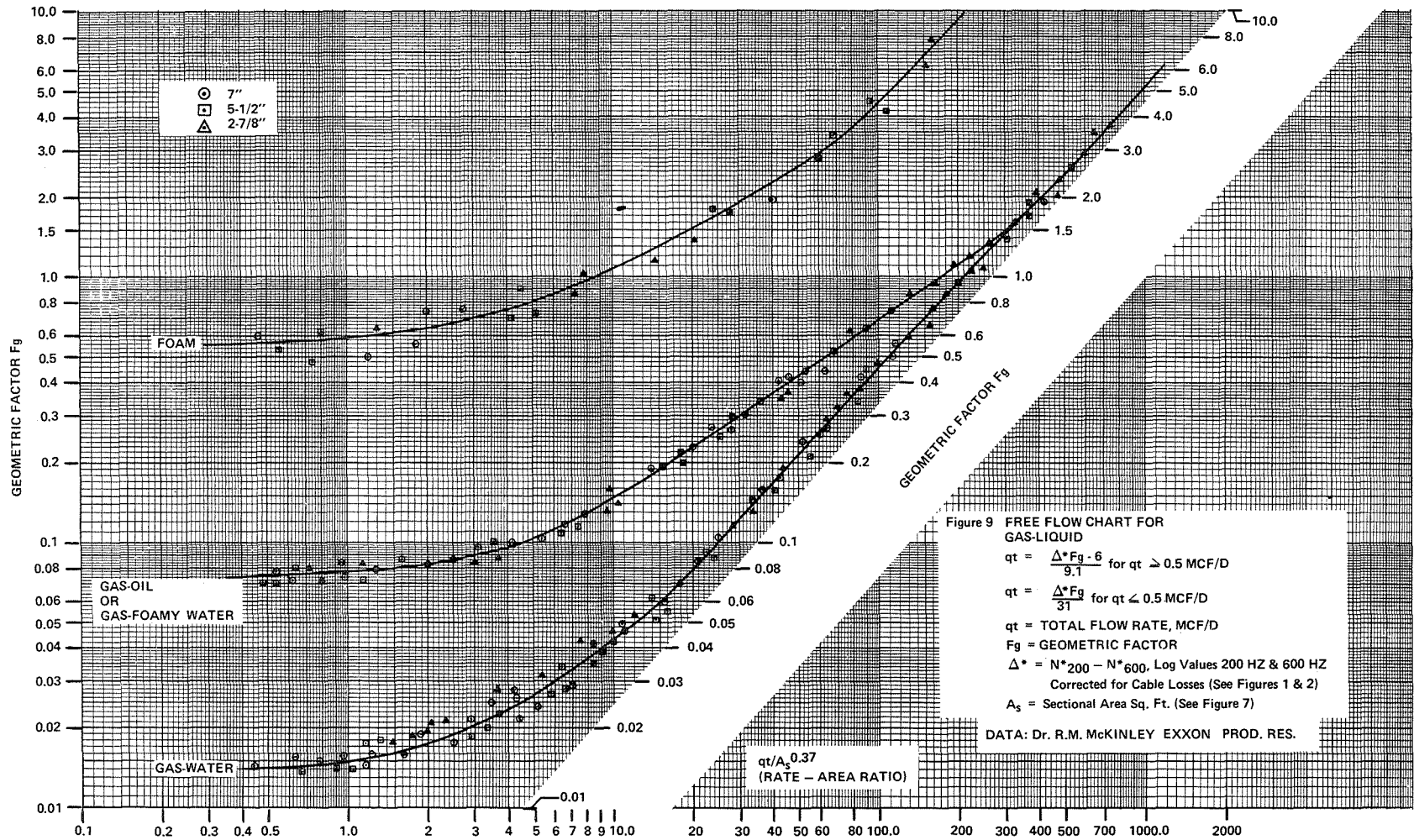


Figure 8 SINGLE PHASE FREE-FLOWCHART
 N*600 = Log Value 600 HZ Corrected for Cable Losses (See Figures 1 & 2)
 A_s = Cross Sectional Area Between Tool and Pipe, Square Feet (See Figure 7)
 F_{fl} = Fluid Loading Factor; 1 for Liquid, 2 for Gas
 ρ = Fluid Density, # /cu. ft.
 qt = Volumetric Flow Rate, MCF/D; Thousands of cu. ft. per day. For Water Flow q_w = 0.178 qt
 R_e = Reynold's Number, Dimensionless
 D_e = D pipe - D tool, ft. (See Figure 7)
 V = Flow Velocity, ft. / Sec.
 μ = Viscosity, #/ft. sec. = Centipoise x 0.000672
 ○ = Air □ = Water X = Diesel Oil
 DATA: Dr. R.M. MCKINLEY EXXON PROD. RES.



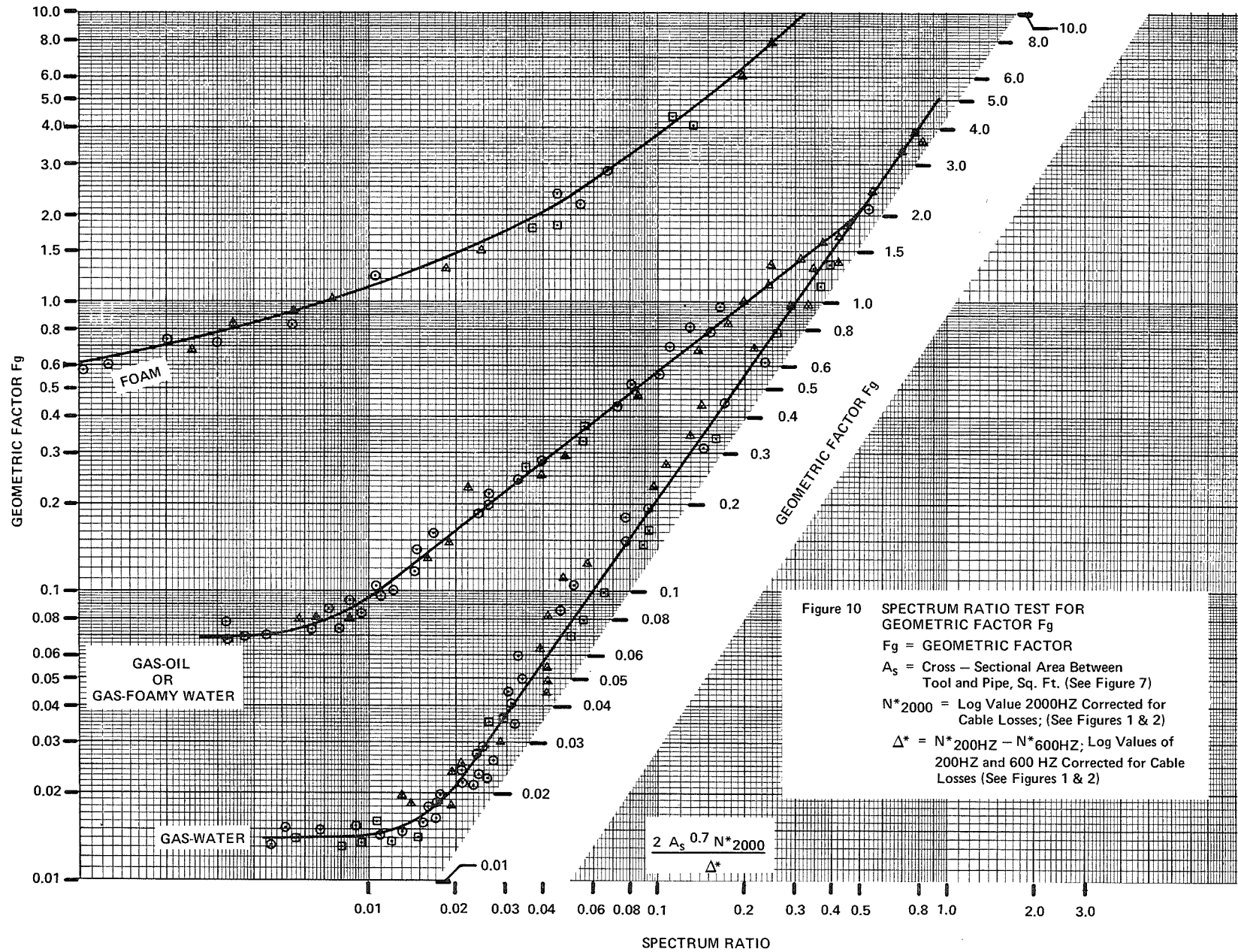


Figure 10 SPECTRUM RATIO TEST FOR GEOMETRIC FACTOR F_g
 F_g = GEOMETRIC FACTOR
 A_s = Cross - Sectional Area Between Tool and Pipe, Sq. Ft. (See Figure 7)
 N^{*2000} = Log Value 2000HZ Corrected for Cable Losses; (See Figures 1 & 2)
 Δ^* = $N^{*200HZ} - N^{*600HZ}$, Log Values of 200HZ and 600 HZ Corrected for Cable Losses (See Figures 1 & 2)